

# GeoArch

Report 2009/18

Archaeometallurgical residues from  
Llynfi Vale Ironworks, Maesteg

Dr Tim Young  
2<sup>nd</sup> July 2009

# Archaeometallurgical residues from Llynfi Vale Ironworks, Maesteg

Dr T.P. Young

## Abstract

*Excavations at Llynfi Vale Ironworks revealed large quantities of slag, particularly blast furnace slag and puddling slag. Little, if any, of this material occurred in contexts which could be linked directly to activities within the site, with much of this material present as make-up deposits which may have brought in from outside the works. Archaeometallurgical investigations were therefore focused on deposits of micro-residues which were associated with use of the ironworks and which were particularly located in areas outside the buildings.*

*The deposits of micro-residues were variably cemented; locally being loose, friable deposits, but elsewhere concretioned into ferricrete horizons which required breaking with mechanical excavators. The dominant particles present were spheroidal hammerscale, with lesser quantities of flake hammerscale, fragmented slag and fuel debris. Cementation was influenced, at least in part, by the local presence of pieces of iron.*

*Analysis of the spheroids indicates that they derive from the shingling of "wet" puddled iron; the first analytical description of such material. The chemical composition, mineralogy and microstructure of the spheroidal hammerscale are quite distinct from that produced during smithing of wrought or bloomery iron. The spheroids are large, mainly in the range 0.5-1.5mm diameter. They are mainly vesicular, often with a blistered surface and occur both with and without a large central cavity. The dominant identifiable iron oxide in the scale is usually magnetite (typically only an accessory mineral in spheroidal hammerscale from smithing); wustite is present in much lower proportions. The spheroidal scale is characterised by high proportions of iron sulphide (up to 10wt%) and also by high concentrations of phosphorus (1.6-2.6 wt% P). Details of the mineralogy of this extremely fine-grained material are obscure, although the similarities with puddling slags are striking. The materials differ from available analyses of puddling slags in being relatively aluminous, probably a reflection of the nature of the fettling employed at this works.*

## Contents

Abstract	1
Methods	1
Background	2
Results	2
1. Spheroidal hammerscale	
1a. Morphology	2
1b. Mineralogy and microstructure	2
1c. Chemical composition	3
2. Flake hammerscale	3
3. Slag	
3a. Mineralogy and microstructure	3
3b. Chemical composition	4
Interpretation	4
Summary	5
References	6
Figure Caption	7
Plate Captions	8
Tables	9

## Methods

All materials were examined visually with a low powered binocular microscope as part of the assessment (Young 2007), following a similar assessment of material from the evaluation excavations (Young 2005) and a database of all materials produced. The assessment identified a particularly interesting series of deposits formed largely of spheroidal hammerscale. A follow-up programme of analysis was designed to investigate the residues in more detail. This report focuses on that material.

Electron microscopy was undertaken on the LEO S360 analytical electron microscope in the School of Earth, Ocean and Planetary Sciences, Cardiff University. Microanalysis was undertaken using the system's Oxford Instruments INCA ENERGY energy-dispersive x-ray analysis system (EDX). All images of microstructures presented in this report are backscattered electron (BSEM) photomicrographs. The polished blocks for investigation on the SEM were prepared in the Earth Science Department, The Open University.

Chemical analysis was undertaken using two techniques. The major elements (Si, Al, Fe, Mn, Mg, Ca, Na, K, Ti, and P) were determined by X-Ray Fluorescence using fused beads, on the Open

University Earth Science Department's Wavelength-Dispersive X-Ray Fluorescence (WD-XRF) system.

Whole-specimen chemical analysis for minor and trace elements (Sc, Ti, V, Cr, Mn, Fe, Co, Zn, Ga, Rb, Sr, Y, Zr, Nb, Mo, Sn, Cs, Ba, La, Ce, Pr, Nd, Sm, Eu, Gd, Tb, Dy, Ho, Er, Tm, Yb, Lu, Hf, Ta, Pb, Th and U) was undertaken using samples in solution on the ThermoElemental X-series Inductively-Coupled Plasma Mass Spectrometer (ICP-MS) in the School of Earth, Ocean and Planetary Sciences, Cardiff University. All sample batches for chemical analysis are run with internationally certified standards.

The examined material was drawn from Sample 4 from Context 148. This was sub-sampled as: (LVI-1) a sample of the indurated scale deposit for investigation by SEM, (LVI-2) a sample of a small slag clast for investigation by SEM and (LVI-3) a collection of isolated pieces of spheroidal hammerscale which was investigated by SEM and through a bulk chemical analysis. Bulk analytical results are presented in Table 4. Microanalytical results are presented in tables 1 and 2. Sample locations for microanalysis are indicated in the relevant BSEM images (Plates 1-7).

## Background

The processes undertaken at the Llynfi Vale Ironworks were typical of those undertaken at many South Wales ironworks specialising in the production of wrought iron rails. The initial smelting of iron ores was undertaken in a range of blast furnaces to the south and southwest of the excavated area. The product of the smelting would have been cast iron (pig iron), a form of iron rich in carbon. Removal of carbon (and other impurities such as silicon, sulphur and phosphorus) was undertaken in the puddling processes. In puddling the iron pigs were reheated in a reverberatory furnace to oxidise the impurities. The puddling process most commonly employed in South Wales was wet puddling (Percy 1864), in which the base of the furnace was lined (fettled) with oxygen-rich material, typically scale or calcined slag, but also sometimes including haematitic iron ore. Oxygen from the fettling reacted with the carbon in the melted pig iron to produce rapid production of carbon monoxide, inducing the appearance of boiling to the melt in the furnace. As the carbon became burnt out of the melt, iron began to solidify. This was worked by the puddler and at the end of the reaction he divided the iron mass into balls of a size suitable for consolidation.

The consolidation process (shingling) could be undertaken either under a steam hammer or in a squeezer. Llynfi Vale Ironworks apparently used a crocodile squeezer for the shingling process. The shingling welds the hot raw iron into a coherent mass, squeezing most of the entrained slag. Some of the slag would be expelled as small molten droplets (spheroidal hammerscale), some as more discrete slag lumps and some would remain inside the iron, forming the characteristic slag inclusions of wrought iron.

The shingled iron billet would then be able to be further worked using a hammer, or as at Llynfi Vale, using rollers to draw-out and form the iron to the required shape.

The old analyses use various terms for puddling slags which need some explanation:

*Mill cinder*: a general term for puddling slags

*Boilings*: slags from the boiling stage of wet puddling, which may overflow the hearth because of the bulk volume increase during the rapid generation of carbon monoxide.

*Tappings*: slag deliberately tapped from the puddling hearth to clear the puddled iron balls.

*Best Tap*: slag from the reheating furnace

*Bulldog*: tapped puddling slag that has been calcined to enhance its use in fettling. It appears that the calcining temperature was sometimes sufficient for a partial melting, enabling liquation of a siliceous component, leaving a magnetite-rich material.

## Results

The upper deposits over the south western part of the excavated site were dominated by spheroidal hammerscale in a variably indurated deposit, which was particularly strongly cemented by secondary iron minerals in areas where the deposits contained iron artefacts. The deposit also contained fine-grained slag, flake hammerscale and fuel debris, amongst other materials. The following sections detail the various components that were investigated from this deposit.

### 1. Spheroidal hammerscale

#### 1a Morphology

Although much of the finer grained spheroidal hammerscale was of high sphericity, there were grains at all size grades, but particularly the larger sizes, which departed markedly from this (in so far as can be determined in 2d section). Lower sphericity grains included varieties with an elongate protrusion and examples with a flattened face.

The investigated grains ranged up to about 3mm diameter. They show a range of internal morphology from grains with almost no vesicularity (e.g. Plate 1g, 3d, 3f), to varieties with a vesicular slag shell surrounding a central cavity (e.g. Plate 2a, 6g). Several grains (particularly amongst the isolated examples examined) showed vesicles concentrated at the margin giving the hammerscale an irregular, blistered, appearance (e.g. Plate 6a, 6e, 6g, 6h). Probably slightly less than half of the spheroids were hollow.

#### 1b Mineralogy and microstructure

The spheroidal particles exhibit a range of microstructures, with a spectrum of textures and mineralogy. Some grains may be dominated by just one part of that spectrum, but most exhibit a range of textures between crust and core. The primary phases in all microstructures were iron oxides. In different microstructures, however, the oxide present was variously magnetite or wustite, or both.

For almost all grains the crust is formed by a thin layer of subhedral equant iron oxide, probably magnetite of close to end member composition (Plate 1f, 2e, 6d, 7f). Immediately inside the crust most spheroids exhibit a layer with isolated euhedral equant magnetite with aluminous cores (up to 24% hercynite). The zone of equant magnetite in glass is often associated with the blistered layer. Inwardly, there are increasing

quantities of iron oxide in a platy or lamellar morphology. This mineral was difficult to analyse because of the narrow width of the plates. Data from the analysis of this phase (and of morphologically similar material in the slag, see below) show an atomic Si:Al ratio of close to 2:1 (Figure 1), with total silica plus alumina ranging up to about 8wt%. This pattern is unlikely to represent substitution in an iron oxide, but may suggest that lamellae include an aluminosilicate. For some spheroids the plates appear to be randomly oriented, but in others the plates become structured inwardly, apparently mimicking the form of a dendrite (Plate 7a). The component strands of the "dendrites" in this microstructure are formed of lamellae, with a composite width of 2-4µm. These composite dendrites contain distinct electron-dense "nodes", which EDS analysis suggests are an iron oxide with low levels of substitution and which are probably wustite.

In some specimens true magnetite dendrites are present, but in most the lamellae grade inwards towards dendrites of wustite.

The iron oxides are set in a groundmass that is mostly apparently glassy, although crystallites are visible in some areas. Analyses of the interstitial material include one that is apparently of an olivine (though slightly too silicic; further discussed below), but most appear to either be of glass or a finely divided mixture of phases. The phosphate content of the interstitial material is high, ranging up to 4.4 atom% P. The recorded sulphur content of the interstitial material is extremely variable (0.2 – 6.9 atom%), which probably indicates that the sulphur is dominantly in the discrete sulphide blebs which were too fine to be imaged, rather than evenly distributed in an interstitial glass.

Throughout the various textures but particularly amongst the lamellar oxide, lie abundant larger (up to 3µm, but the majority <1µm) blebs of iron sulphide. Analyses of these blebs suggest an Fe:S ratio of approximately 1.4, close to that of an unknown iron sulphide phase reported by Killick and Gordon (1987) from examples of puddling slags.

### 1c Chemical composition

EDS analyses of areas within the various components of the assemblage are given in Table 2 with a summary of the average composition in Table 3. The data are normalised to allow comparison between areas of differing vesicularity.

The different textures of spheroidal particles show bulk compositions close to each other and to that of some of the small slag particles, although the larger slag specimen (LVI-2) contains distinctly more silica and alumina, and has a lower sulphur content.

The spheroid compositions mainly fall in the range of 3-5wt% Al<sub>2</sub>O<sub>3</sub>, 7-14% SiO<sub>2</sub>, 3.5-6.5% P<sub>2</sub>O<sub>5</sub>, 1-3%S, <0.4%K<sub>2</sub>O, <1.5%CaO and <0.8%MnO with the remainder iron as oxide or combined with the S.

The alumina to silica ratio is very high compared with other examples of puddling slags, although similar to the slag sample analysed in this project (average ratio 0.39 for spheroids, 0.40 for the slag LVI-2).

The sulphur content is high (2.09 wt% S on average), corresponding to 7.12 wt% of the phase Fe<sub>1.4</sub>S.

## 2. Flake hammerscale

The indurated sample LVI-1 contained a few small fragments of granular iron oxide which appeared to be small chips of flake hammerscale. The paucity of such fragments suggests that the process generating the spheroidal scale produced rather little flake scale, or that the two classes of material have become separated. This would be the case if the deposits were receiving fines from the squeezer, but not from the rolling mill.

The analysed particles show a simple granular morphology, with low levels of substitution in the wustite.

## 3. Slag

### 3a Mineralogy and microstructure

A small isolated slag fragment from the scale deposit was examined (LVI-2), as were several small slag fragments within the sample of the cemented deposit (LVI-1).

#### LVI-1:

The fragments from LVI-1 are very small, but include an example of a slag showing a cooling front (possibly a fragment of a tapped puddling slag) and a more homogeneous example. Neither of these slag fragments was examined in detail. Both had dendritic microstructures dominated by wustite. The example with the cooling front showed very similar altered foliations to those seen and analysed in detail in LVI-2.

#### LVI-2:

The slag LVI-2 shows an unusual foliated microstructure which is interpreted as representing fractures induced by brittle deformation, probably produced by the crusher.

The primary phase in the slag comprises a generation of sparse, stubby wustite dendrites. These are apparently overgrown in some areas (although the distribution is slightly exclusive) by a lamellar iron oxide which appears to be magnetite.

The main groundmass phase is olivine, in a small scale microstructure of disrupted appearance. This may indicate that the deformation suffered by this sample occurred before complete solidification of the olivine. The olivine appears to be a fayalite which shows low levels (<2%) of substitution with Ca, Mn and Mg. The analyses do not, however, correspond precisely with olivine, having too much silica in the analyses, together with up to 2.6 atom% P. This probably suggests that olivine is significantly altered, although it is possible the olivine contains inclusions of other phases not resolved by the BSEM image.

The olivine and iron oxides are both overgrown by a small quantity of a symplectic intergrowth of wustite with a material of low electron density. Analysis of this material is difficult because of its very fine grain size, but although the textures resemble those of a symplectic leucite-wustite intergrowth the analyses undertaken do not indicate leucite, but rather a glass or weathering-product.

The specimen is cut by two sets of foliations. Firstly an early set of sub-parallel cracks, filled by material of low-electron density (dark on plate 5a-d). EDS shows these veins to be of iron phosphate with minor aluminium, a Fe:P atomic ratio of 1.3-1.5 and an

analytical total of 60-70 wt% , indicating a hydrated material of vivianite-like composition. This suggests that this material is secondary. The morphology of the foliations suggests either an origin through shock, or just possibly that they are pseudomorphs of an early crystalline phase forming platy crystals of large dimensions.

The second set of foliations is less regular and is indicative of later stage brittle fracturing.

### 3b. Chemical composition

The bulk chemical composition of the slag LVI-2 was determined by EDS analysis of a representative area (tables 1 and 3). The analysis is richer in Si and Al than the spheroidal hammerscale, but they occur in the same ratio. P is extremely high (reflecting the abundant iron phosphate in the foliations); S was below detection.

The key features of this analysis are therefore the low sulphur content and the aluminous composition. The aluminous composition is shared with the spheroids (Table 3), but the low sulphur is not. It seems unlikely that the sulphur has been lost during the weathering of this sample (the weathering materials are themselves sulphur-poor), so it seems a primary feature of this slag.

## Interpretation

There are very few analytical investigations of hammerscale, even fewer of puddling slags and none known to the author of hammerscale from the shingling of puddled iron. This present investigation is therefore significant, but at the same time, the scope of possible comparative material is therefore very limited.

The chemical composition and microstructure of spheroidal hammerscale has been examined in a few recent studies, all of which were from manual blacksmithing. The first detailed observations of the morphology of spheroidal hammerscale were presented by Allen (1986) in a morphological classification of fines from Romano-British smithing at Awre (Gloucestershire, England). Although Allen's study was not mineralogical, he comments that the air-chilled and surface chilled spatter (equivalent to spheroidal hammerscale) were "fayalitic, with silica contents similar to or somewhat less than the associated smelting slags" (which was 16-36 wt%, average 24%, according to the data presented by Allen & Fulford 1987) and the bloom scale and contact scale (equivalent to flake hammerscale) were "almost pure iron oxide (chiefly or wholly magnetite)".

19th century blacksmithing fines from Bixby blacksmith's shop (Barre Four Corners, Massachusetts, USA) were examined by Unglik (1991), who examined the microstructure and mineralogy of a variety of materials. He identified two main morphologies (globules and plates) with three recurrent microstructures, referred to granular, dendritic and fused microstructures respectively. His "smithing globules" (0.1 to 4.2mm diameter) and "smithing scales" are described as both being iron-rich (approximately 60 wt% iron, equivalent to 80 wt% calculated as FeO). Two thirds of the globules were hollow. Larger globules were less perfectly spheroidal than smaller ones.

Dungworth and Wilkes (2007) have argued that the chemical composition of hammerscale in their

experiments was largely controlled by the composition of the slag inclusions in the metal. It is apparent from their data, however, that the silica:alumina ratio of the hammerscale is slightly lower than that of the slag inclusions. Clearly some modification of the silicate component has taken place, though whether through mixing or fractionation is not apparent. They comment that "most" spheroidal hammerscale from their welding experiments was hollow.

Two currently unpublished reports have approached the study of hammerscale using broadly the same methodology adopted here. Young (2008) examined an assemblage of early medieval age from Coolamurry, Co. Wexford. The Coolamurry assemblage documents the generation of silicate slags within a relatively silicate-poor system, with a charcoal-fired hearth blown through a ceramic tuyère. Promotion of slag generation may have been achieved through deliberate addition of a welding flux. Despite this possible use of flux, the hammerscale particles are extremely iron-rich. Indeed, the spheroidal hammerscale is more iron-rich than perhaps would be expected from the current literature. Whether this is a failing in the current literature, or whether spheroidal hammerscale produced during the working of iron heated in a hearth with a ceramic tuyère is more iron-rich than that produced in a clay-lined hearth with a blowhole, remains to be determined.

In contrast, Young (2009) described residues from a coal-fired hearth, probably blown through a simple blowhole, of Romano-British age, from Trowbridge, Cardiff, Wales. A low silica:alumina ratio for the hammerscale at Trowbridge was interpreted as reflecting the influence of the relatively aluminous coal ash, supporting a model where the influence of external silicate materials assists in the generation of the hammerscale.

At both Coolamurry and Trowbridge the dominant iron oxide the spheroidal hammerscale is wustite, although at both localities there are spheroids which show some primary magnetite, and secondary oxidation of the outer parts of spheroids to magnetite was noted at Coolamurry. At Coolamurry the silicates (mainly olivine and glass) formed a significant component of the microstructure, but at Trowbridge the iron oxides were predominant. This is a reflection of a higher iron content of the residues at Trowbridge, with a total of silica and alumina for flake scale of 4.3wt% (Coolamurry: 5-8wt%) and for spheroidal scale of 6.7-7.2wt% (Coolamurry: c.15wt%).

The previous studies of manual blacksmithing microresidues therefore present spheroidal hammerscale as having a range of iron contents, depending upon the originating process and the hearth chemistry, but with the iron dominantly in reduced state in wustite and fayalite. Minor secondary oxidation to magnetite is seen, alongside some rare particles with primary magnetite.

In contrast the spheroids from Llynfi Vale Ironworks are rather more oxidised, with a restricted significance for wustite and with much more magnetite. The platy iron oxide in the spheroids is of uncertain nature, but appears part of the crystallization texture. In contrast, the apparently rather similar oxides in the slag specimen show a foliated texture with frayed tips, which may be an alteration texture, suggesting that these crystals were arrested in the process of reaction – and might therefore be related, in their original state, to the fettling material. These particles show an average  $Al_2O_3:SiO_2$  of 0.48 and so have the possibility

of being linked strongly with the bulk  $\text{Al}_2\text{O}_3:\text{SiO}_2$  ratio (0.40 for the slag and 0.39 for the spheroids, measured by EDS). Whilst the lamellar oxide appears to be of the same electron density as the magnetite, and generally does not show a lower analytical total than the magnetite (with both calculated with iron as FeII), the lamellar habit of the mineral more strongly resembles that of haematite.

Within the scope of a fairly small sample size the spheroids showed a rather similar range of overall morphology to the previously-described assemblages of spheroidal hammerscale, although the blistered, magnetite-rich, vesicular surface layer is a distinguishing feature.

The bulk compositions of the different textures of spheroid are fairly similar. Overall iron content, quoted as FeO, would be 74.3 wt% for the slag sample, 79.0 wt% for the dense spheroids, 74.5 for the dense vesicular spheroids and 75.7 wt% for the hollow spheroids. The total of alumina + silica is 13-14 wt% for all the different spheroidal particle classes and 2.6% for the flake hammerscale.

All the materials are quite distinct from the dry puddling slags described by Killick & Gordon (1984), which are much more siliceous (having high temperature silica polymorphs as a significant mineralogical component). The Llynfi Vale material also contains very much more sulphur and phosphorus than the dry puddling samples.

One interesting point of similarity with the analyses of Killick & Gordon is the curious composition of the iron sulphide, equivalent to about  $\text{Fe}_{1.4}\text{S}$ . This composition is very close to the sulphide blebs (a product of liquid immiscibility) recorded in the broadly olivine composition glass of the white cast iron-bearing igneous dykes on Disko, Greenland (Pedersen 1979; Ulff-Møller 1985) and is also close to ternary eutectic iron-wüstite-troilite composition recorded by Naldrett (1969). It is therefore likely that these grains represent a eutectic mixture, rather than a single mineral.

The spheroids bear a close relationship to the accompanying slag fragment, but differ in having lower alumina and silica contents, but higher sulphur.

The aluminous composition of both spheroids and slag is presumably inherited from the fettling material rather than from the pig iron. Percy's (1864) account of the material sometimes employed (albeit in Staffordshire) as a fluxes and fettling mentions:

*Puddling mine (roasted Staffordshire Red mine)*  
*Red haematite*  
*Bulldog*  
*Scrap iron*

And the charge may contain:

*Refined iron*  
*Pig iron*  
*Mill scale*  
*Hammer slag*

In earlier puddling techniques he mentions a fluxes formed of:

*Common salt*  
*Nitre*  
*White fireclay*  
*Manganese oxide*  
*Haematite ore*  
*Unslaked lime*  
*Charcoal powder*

Apart from the fireclay here is little in any of these ingredients that might be expected to be particularly aluminous. On the other hand, residues from burning coal are typically aluminous (e.g. Young 2009 for analysis of relatively local material), so it is possible the slag composition has been influenced by the coal ash composition, via one of the fettling materials.

## Summary

This study provided the first description of spheroidal hammerscale from the shingling of puddled iron. Considerable uncertainty remains over the precise nature of some of the iron oxide phases, but none the less there are striking parallels between the spheroidal hammerscale and published accounts of puddling slags on the one hand and a marked dissimilarity with spheroidal hammerscale from blacksmithing on the other.

The shingling of a puddled iron ball is a much simpler system than blacksmithing. The ball has been removed from its associated molten slag bath, but the entrained slag should be largely representative of that bath. The agitation of the ball in the slag as it forms should have produced a good level of homogeneity in the slag, although slag trapped and isolated within the spongy ball might evolve in a way which deviated from the bulk slag in the bath. The continued heating of the ball after its formation (typically on the fire bridge of the puddling furnace) might have entailed a little re-oxidation of the adhering slag if the hearth was run too fiercely, but ideally the shingling would be expected to be expelling slag from the ball that would be close in composition to that in the furnace.

The composition of the spheroidal hammerscale corresponds to historical analyses of slags from wet puddling. The scale differs from the modern analytical studies of Killick and Gordon (1987) on dry puddling residues in lacking free silica.

The spheroidal scale differs markedly from previously-described spheroidal hammerscale from blacksmithing. This suggests that detailed observations of spheroidal hammerscale within modern ironworks may be capable of resolving spheroids from different stages of the manufacturing process.

## References

- ALLEN, J.R.L. 1986. Interpretation of some Romano-British smithing slags from Awre, Gloucs. *Historical Metallurgy*, **20**, 97-104.
- ALLEN, J.R.L. & FULFORD, M.G. 1987. Romano-British settlement and industry on the wetlands of the Severn Estuary. *Antiquaries Journal*, **62**, 237-289.
- DUNGWORTH, D. & WILKES, R. 2007. *An Investigation of Hammerscale*. Research Department Reports Series No. 26/2007, English Heritage, 36pp.
- HEARSON, H.R. 1922. *The manufacture of iron and steel*. Spon, London.
- KILLICK, D.J. & GORDON, R. B. 1987. Microstructures of puddling slags from Fontley, England, and Roxbury, Connecticut. *Historical Metallurgy*, **21**, 28-36.

MACFARLANE, W. 1917. *The Principles and Practice of Iron and Steel Manufacture*. Longmans, London, 253pp.

NALDRETT, A.J., 1969. A portion of the system Fe-S-O between 900 and 1080 °C and its application to sulfide ore magmas. *Journal of Petrology*, **10**, 171-201.

PEDERSEN, A. K., 1979b. Basaltic glass with high-temperature equilibrated immiscible sulphide bodies with native iron from Disko, central West Greenland. *Contributions to Mineralogy and Petrology*. **69**, 397-407.

PERCY, J. 1864. *Metallurgy: The art of extracting metals from their ores, and adapting them to various purposes of manufacture.*, *Iron and Steel*. London, John Murray, 934pp.

STANSBIE, J.H. 1907. *Iron and Steel*. London

STARLEY, D. 1995. *Hammerscale*. Historical Metallurgy Society, Archaeological Datasheet no. 10.

ULFF-MØLLER, F. 1985. Solidification history of the Kitdilt Lens; immiscible metal and sulphide liquids from a basaltic dyke on Disko, central West Greenland. *Journal of Petrology*, **26**, 64-91

YOUNG, T.P. 2005. Metallurgical residues and structures from an evaluation at Llynfi Ironworks, Maesteg. *GeoArch Report 2005/01*. 2pp.

YOUNG, T.P. 2007. Evaluation of archaeometallurgical residues from Llynfi Ironworks. *GeoArch Report 2007/25*. 3pp.

YOUNG, T.P. 2008. Archaeometallurgical residues from Coolamurry 7, 04E0323. *GeoArch Report 2006/10*. 46pp.

YOUNG, T.P. 2009. Archaeometallurgical residues from Crickhowell Road, Trowbridge, Cardiff. *GeoArch Report 2009/02*.

## Figure Caption

Figure 1. Plot of SiO<sub>2</sub> v Al<sub>2</sub>O<sub>3</sub> for EDS analyses of phases from samples LVI-1/3 (spheroids) and LVI-2 (slag).

## Plate Captions

### Plate 1. BSEM images of LVI-1

- a. Area 1, scale bar 600 $\mu$ m
- b. Area 2, scale bar 100 $\mu$ m
- c. Area 3, scale bar 100 $\mu$ m
- d. Area 4, scale bar 100 $\mu$ m
- e. Area 5, scale bar 1mm
- f. Area 6, scale bar 100 $\mu$ m
- g. Area 7, scale bar 400 $\mu$ m
- h. Area 8, scale bar 100 $\mu$ m

### Plate 2. BSEM images of LVI-1

- a. Area 9, scale bar 800 $\mu$ m
- b. Area 10, scale bar 100 $\mu$ m
- c. Area 24, scale bar 100 $\mu$ m
- d. Area 31, scale bar 600 $\mu$ m
- e. Area 32, scale bar 70 $\mu$ m
- f. Area 33, scale bar 60 $\mu$ m
- g. Area 34, scale bar 1mm
- h. Area 35, scale bar 1mm

### Plate 3. BSEM images of LVI-1

- a. Area 36, scale bar 1mm
- b. Area 17, scale bar 400 $\mu$ m
- c. Area 18, scale bar 300 $\mu$ m
- d. Area 19, scale bar 100 $\mu$ m
- e. Area 20, scale bar 200 $\mu$ m
- f. Area 21, scale bar 400 $\mu$ m
- g. Area 22, scale bar 100 $\mu$ m
- h. Area 23, scale bar 600 $\mu$ m

### Plate 4. BSEM images of LVI-1

Montage comprises areas 11-16 and 25-30.  
Scale bar 3mm

### Plate 5. BSEM images of LVI-2

- a. Area 1, scale bar 1mm
- b. Area 2, scale bar 100 $\mu$ m
- c. Area 3, scale bar 60 $\mu$ m
- d. Area 4, scale bar 400 $\mu$ m

### Plate 6. BSEM images of LVI-3

- a. Area 2, scale bar 2mm
- b. Area 3, scale bar 100 $\mu$ m
- c. Area 4, scale bar 2mm
- d. Area 5, scale bar 100 $\mu$ m
- e. Area 6, scale bar 2mm
- f. Area 7, scale bar 100 $\mu$ m
- g. Area 8, scale bar 2mm
- h. Area 9, scale bar 100 $\mu$ m

### Plate 7. BSEM images of LVI-3

- a. Area 10, scale bar 40 $\mu$ m
- b. Area 11, scale bar 2mm
- c. Area 12, scale bar 100 $\mu$ m
- d. Area 13, scale bar 2mm
- e. Area 14, scale bar 100 $\mu$ m
- f. Area 15, scale bar 100 $\mu$ m

Plate 8. Backscattered electron images of materials from Llynfi Vale Ironworks  
(representative material for publication)

a. LVI-2, area 1, scale bar 1mm.  
Image shows the typical texture of the slag fragment. Bright areas are iron oxides, pale grey is dominantly olivine (fayalite) and the dark lineations are phosphate-rich materials in various sub-parallel alignments, together with the fills of late-stage brittle cracks

b. LVI-2, area 2, scale bar 100 $\mu$ m.  
Detail of the area shown in (a). Bright rounded areas are wustite dendrites, pale elongate, foliated areas are iron oxide (magnetite?), pale grey is dominantly olivine (fayalite) and the dark lineations are phosphate-rich materials in various sub-parallel alignments, together with the fills of late-stage brittle cracks

c. LVI-3, area 2, scale bar 2mm.  
Image of grain 3-1, showing central dense but vesicular slag, with marginal vesicles and outer "blistered" crust.

d. LVI-3, area 6, scale bar 2mm.  
Image of grain 3-3, showing central dense slag with a large collapsed vesicle, marginal vesicles and outer "blistered" crust.

e. LVI-3, area 7, scale bar 100 $\mu$ m.  
Detail of texture of grain 3-3 shown in (d). The microstructure is a mesh of plates of lamellar iron oxides in a glassy(?) groundmass. Rounded iron sulphide blebs occur associated with the lamellar oxide.

f. LVI-3, area 9, scale bar 100 $\mu$ m.  
Detail of texture of grain 3-4. This is a vesicular hollow grain with a blistered surface (left of image). This image shows the rather contorted crust overlying a zone with rather equant magnetite (pale) in a glassy groundmass (mid-grey). This zone contains an incomplete crust, represented by a zone of magnetite just to the right of the "blistered" vesicles. Further in to the grain the dominant equant magnetite gives way to a dendritic structure (white), again with an interstitial glass, with some porosity (black).

g. LVI-3, area 10, scale bar 40 $\mu$ m.  
Detail of texture of grain 3-4. The image shows that the dendritic structures visible in (f) are composed of a lamellar oxide, with denser areas at the intersections of the dendrite arms (nodes). The interstitial areas are glass (mid grey), which either incompletely filled the volume or has been etched away, leaving voids (black). Small white blebs are iron sulphide.

h. LVI-1, area 32, scale bar 70 $\mu$ m.  
Detail of the margin of grain 1-14. Upper left is void (black) with a finely layered cement (mid grey) coating the surface of the spheroid. The outer layer is dense, granular oxide (white), probably magnetite. Inside the crust lie equant, euhedral magnetite crystals (white) with hercynite-rich cores (pale grey). The equant magnetite is associated with plates of iron oxide, probably also magnetite. The interstitial material is at least partly crystalline (pale grey) and is probably mainly olvine.

LVI-	SOI	#	Slag	wt% oxide														Total	atom%																
				Mg	Al	Si	P	S	Cl	K	Ca	Ti	V	Cr	Mn	Fe	Fe (S)		O	Mg	Al	Si	P	S	Cl	K	Ca	Ti	V	Cr	Mn	Fe			
2	2	5	wustite	0.00	0.52	0.39	0.00	0.00	0.00	0.00	0.00	0.00	0.31	0.00	0.00	0.00	97.79	0.00	<b>99.02</b>	49.86	0.00	0.37	0.24	0.00	0.00	0.00	0.00	0.00	0.00	0.14	0.00	0.00	0.00	0.18	49.39
2	2	6	wustite	0.00	0.57	0.00	0.00	0.00	0.00	0.00	0.00	0.00	0.29	0.00	0.00	0.34	96.34	0.00	<b>97.55</b>	49.84	0.00	0.41	0.00	0.00	0.00	0.00	0.00	0.00	0.13	0.00	0.00	0.18	49.43		
2	3	2	wustite	0.00	0.72	0.00	0.00	0.00	0.00	0.00	0.00	0.00	0.00	0.00	0.00	0.49	96.66	0.00	<b>97.86</b>	50.10	0.00	0.52	0.00	0.00	0.00	0.00	0.00	0.00	0.00	0.00	0.25	49.13			
2	3	3	wustite	0.00	0.77	1.08	0.43	0.00	0.00	0.00	0.00	0.00	0.00	0.00	0.00	0.35	94.94	0.00	<b>97.57</b>	49.87	0.00	0.55	0.66	0.22	0.00	0.00	0.00	0.00	0.00	0.00	0.18	48.51			
																			<b>49.92</b>	<b>0.00</b>	<b>0.46</b>	<b>0.22</b>	<b>0.06</b>	<b>0.00</b>	<b>0.00</b>	<b>0.00</b>	<b>0.00</b>	<b>0.07</b>	<b>0.00</b>	<b>0.00</b>	<b>0.15</b>	<b>49.11</b>			
2	3	7	wustite (mixed analysis)	0.00	7.35	2.79	0.98	0.00	0.00	0.00	0.22	0.00	0.00	0.00	0.00	87.81	0.00	<b>99.16</b>	55.72	0.00	4.46	1.44	0.43	0.00	0.00	0.00	0.12	0.00	0.00	0.00	0.00	0.00	37.83		
2	2	13	olivine	0.34	1.18	26.60	6.01	0.00	0.00	0.00	0.60	0.00	0.00	0.00	1.03	61.50	0.00	<b>97.26</b>	58.20	0.24	0.67	12.85	2.46	0.00	0.00	0.00	0.31	0.00	0.00	0.00	0.42	24.85			
2	2	14	olivine	0.00	2.91	30.51	4.29	0.00	0.00	0.00	0.47	0.00	0.00	0.00	1.15	52.42	0.00	<b>91.75</b>	61.13	0.00	1.61	14.30	1.70	0.00	0.00	0.00	0.24	0.00	0.00	0.00	0.46	20.56			
2	2	15	olivine	0.31	1.02	29.26	6.46	0.00	0.00	0.00	0.65	0.00	0.00	0.00	1.19	53.66	0.00	<b>92.55</b>	60.60	0.22	0.57	13.89	2.60	0.00	0.00	0.00	0.33	0.00	0.00	0.48	21.31				
2	2	16	olivine	0.00	1.11	30.01	5.95	0.00	0.00	0.00	1.20	0.00	0.00	0.00	1.48	55.33	0.00	<b>95.07</b>	61.61	0.00	0.59	13.53	2.27	0.00	0.00	0.00	0.58	0.00	0.00	0.56	20.86				
2	3	8	olivine	0.35	0.96	30.63	5.56	0.00	0.00	0.00	0.77	0.00	0.00	0.00	1.44	55.57	0.00	<b>95.27</b>	60.31	0.24	0.52	14.22	2.18	0.00	0.00	0.00	0.38	0.00	0.00	0.57	21.58				
2	2	1	magnetite: lamellar	0.00	2.82	5.77	0.33	0.32	0.00	0.00	0.00	0.00	0.00	0.00	0.53	86.43	0.79	<b>96.99</b>	51.51	0.00	1.93	3.35	0.16	0.35	0.00	0.00	0.00	0.00	0.00	0.00	0.26	42.43			
2	2	2	magnetite: lamellar	0.00	3.09	7.97	0.42	0.00	0.00	0.00	0.00	0.00	0.00	0.00	0.57	87.03	0.00	<b>99.07</b>	51.81	0.00	2.06	4.51	0.20	0.00	0.00	0.00	0.00	0.00	0.00	0.00	0.27	41.16			
2	2	3	magnetite: lamellar	0.00	3.39	6.63	0.40	1.64	0.00	0.00	0.00	0.28	0.00	0.00	0.63	81.39	4.01	<b>98.39</b>	50.86	0.00	2.25	3.74	0.19	1.74	0.00	0.00	0.00	0.12	0.00	0.00	0.30	40.80			
2	2	4	magnetite: lamellar	0.00	4.22	7.89	0.41	0.00	0.00	0.00	0.38	0.00	0.00	0.00	0.54	85.19	0.00	<b>98.64</b>	52.34	0.00	2.78	4.41	0.20	0.00	0.00	0.00	0.16	0.00	0.00	0.25	39.85				
2	2	17	magnetite: lamellar	0.00	1.20	2.21	0.00	0.27	0.00	0.00	0.00	0.00	0.00	0.41	91.80	0.67	<b>96.56</b>	50.58	0.00	0.86	1.33	0.00	0.31	0.00	0.00	0.00	0.00	0.00	0.00	0.21	46.72				
2	3	1	magnetite: lamellar	0.00	1.67	3.47	0.00	0.39	0.00	0.00	0.00	0.00	0.00	0.00	0.65	88.95	0.96	<b>96.09</b>	50.33	0.00	1.19	2.10	0.00	0.44	0.00	0.00	0.00	0.00	0.00	0.33	45.61				
2	3	4	magnetite: lamellar	0.00	2.97	7.43	0.49	0.00	0.00	0.00	0.00	0.00	0.00	0.00	0.62	87.00	0.00	<b>98.50</b>	52.62	0.00	1.96	4.16	0.23	0.00	0.00	0.00	0.00	0.00	0.00	0.29	40.74				
																		<b>51.43</b>	<b>0.00</b>	<b>1.86</b>	<b>3.37</b>	<b>0.14</b>	<b>0.41</b>	<b>0.00</b>	<b>0.00</b>	<b>0.00</b>	<b>0.04</b>	<b>0.00</b>	<b>0.00</b>	<b>0.27</b>	<b>42.47</b>				
2	3	9	Symplectic with wustite	0.00	2.53	11.82	11.47	0.32	0.00	0.00	0.63	0.00	0.00	0.00	0.00	33.70	0.78	<b>61.25</b>	55.32	0.00	2.43	9.64	7.91	0.49	0.00	0.00	0.55	0.00	0.00	0.00	0.00	23.66			
2	3	10	Symplectic with wustite	0.00	8.43	12.92	5.67	0.33	0.18	0.00	0.72	0.00	0.00	0.00	0.00	40.22	0.81	<b>69.28</b>	48.65	0.00	7.99	10.39	3.86	0.50	0.24	0.00	0.62	0.00	0.00	0.00	0.00	27.75			
2	3	11	Symplectic with wustite	0.00	6.36	13.11	3.43	0.34	0.13	0.00	0.35	0.00	0.00	0.00	0.00	41.01	0.82	<b>65.55</b>	45.84	0.00	6.78	11.85	2.63	0.57	0.20	0.00	0.34	0.00	0.00	0.00	31.80				
2	3	12	Symplectic with wustite	0.00	3.83	12.43	7.92	0.30	0.13	0.13	0.46	0.00	0.00	0.00	0.34	57.08	0.74	<b>83.36</b>	37.94	0.00	3.79	10.43	5.63	0.48	0.19	0.14	0.42	0.00	0.00	0.24	40.75				
																		<b>46.94</b>	<b>0.00</b>	<b>5.25</b>	<b>10.58</b>	<b>5.01</b>	<b>0.51</b>	<b>0.16</b>	<b>0.03</b>	<b>0.48</b>	<b>0.00</b>	<b>0.00</b>	<b>0.06</b>	<b>30.99</b>					
2	2	7	Iron phosphate	0.00	3.42	0.88	22.87	0.34	0.14	0.31	1.24	0.00	0.00	0.00	0.00	29.53	0.83	<b>59.57</b>	64.85	0.00	2.70	0.59	12.97	0.43	0.16	0.26	0.89	0.00	0.00	0.00	0.00	17.15			
2	2	8	Iron phosphate	0.00	3.09	0.00	30.20	0.39	0.00	0.32	0.75	0.00	0.00	0.00	0.00	35.75	0.96	<b>71.45</b>	67.93	0.00	1.88	0.00	13.20	0.38	0.00	0.21	0.41	0.00	0.00	0.00	0.00	15.98			
2	2	9	Iron phosphate	0.00	7.41	0.79	23.00	0.36	0.00	0.22	1.11	0.00	0.00	0.00	0.00	31.48	0.88	<b>65.25</b>	65.22	0.00	5.20	0.47	11.59	0.40	0.00	0.17	0.71	0.00	0.00	0.00	0.00	16.24			
2	2	11	Iron phosphate	0.00	3.07	0.00	17.46	0.27	0.00	0.20	0.73	0.00	0.00	0.00	0.00	28.60	0.66	<b>50.99</b>	63.21	0.00	2.99	0.00	12.20	0.42	0.00	0.21	0.65	0.00	0.00	0.00	20.33				
2	2	12	Iron phosphate	0.00	4.31	1.70	29.77	0.36	0.00	0.25	3.11	0.00	0.00	0.00	0.00	32.64	0.87	<b>73.01</b>	68.66	0.00	2.46	0.82	12.24	0.33	0.00	0.15	1.62	0.00	0.00	0.00	13.71				
2	2	18	Iron phosphate	0.00	4.50	1.18	20.49	0.53	0.12	0.18	1.69	0.00	0.00	0.00	0.00	27.50	1.30	<b>57.48</b>	63.68	0.00	3.74	0.83	12.24	0.71	0.14	0.16	1.28	0.00	0.00	0.00	17.22				
2	2	19	Iron phosphate	0.00	3.36	0.79	24.88	0.38	0.00	0.20	0.76	0.00	0.00	0.00	0.00	34.82	0.93	<b>66.12</b>	66.51	0.00	2.30	0.46	12.23	0.41	0.00	0.15	0.47	0.00	0.00	0.00	17.48				
																		<b>65.72</b>	<b>0.00</b>	<b>3.04</b>	<b>0.45</b>	<b>12.38</b>	<b>0.44</b>	<b>0.04</b>	<b>0.19</b>	<b>0.86</b>	<b>0.00</b>	<b>0.00</b>	<b>0.00</b>	<b>0.00</b>	<b>16.87</b>				
2	2	10	Contaminated?	0.00	29.11	1.24	1.45	0.33	1.15	0.00	0.91	0.00	0.00	0.00	1.96	0.80	<b>36.95</b>	56.91	0.00	34.53	1.25	1.23	0.62	1.95	0.00	0.98	0.00	0.00	0.00	0.00	2.52				
2	3	5	Mixed fayalite/phosphate?	0.00	2.66	11.65	20.09	0.71	0.11	0.33	0.83	0.00	0.00	0.00	0.00	34.07	1.74	<b>72.18</b>	64.34	0.00	1.72	6.39	9.34	0.73	0.10	0.23	0.49	0.00	0.00	0.00	16.66				
																		<b>60.63</b>	<b>0.00</b>	<b>18.12</b>	<b>3.82</b>	<b>5.29</b>	<b>0.68</b>	<b>1.03</b>	<b>0.11</b>	<b>0.73</b>	<b>0.00</b>	<b>0.00</b>	<b>0.00</b>	<b>9.59</b>					
3	10	2	Spheroids glass	0.00	5.51	21.53	8.81	3.00	0.00	0.59	3.63	0.00	0.00	0.00	0.95	52.08	7.31	<b>103.42</b>	55.46	0.00	2.95	9.79	3.39	2.55	0.00	0.34	1.77	0.00	0.00	0.37	23.38				
3	12	3	magnetite	0.00	0.98	0.83	0.00	1.08	0.00	0.00	0.00	0.00	0.00	0.00	94.47	2.64	<b>100.01</b>	51.41	0.00	0.65															

SOI	#		wt% oxide													Total	atom%																
			Mg	Al	Si	P	S	Cl	K	Ca	Ti	V	Cr	Mn	Fe		Fe (S)	O	Mg	Al	Si	P	S	Cl	K	Ca	Ti	V	Cr	Mn	Fe		
1	33	4	magnetite: equant grain	0.00	13.18	0.52	0.00	0.00	0.00	0.00	0.00	0.49	0.51	0.81	0.00	80.16	0.00	<b>95.66</b>	55.85	0.00	8.12	0.27	0.00	0.00	0.00	0.00	0.00	0.00	0.19	0.17	0.33	0.00	35.06
3	7	4	magnetite or wustite node	0.00	1.63	0.96	0.37	0.27	0.00	0.00	0.00	0.00	0.00	0.00	0.00	97.50	0.67	<b>101.40</b>	51.77	0.00	1.08	0.54	0.17	0.29	0.00	0.00	0.00	0.00	0.00	0.00	0.00	46.15	
3	10	3	magnetite: lamellar/node	0.00	1.95	0.85	0.00	0.28	0.00	0.00	0.00	0.00	0.00	0.00	0.00	96.90	0.68	<b>100.66</b>	52.58	0.00	1.27	0.47	0.00	0.29	0.00	0.00	0.00	0.00	0.00	0.00	0.00	45.38	
1	33	15	magnetite: lamellar (mixed?)	0.00	1.72	10.63	6.56	3.89	0.00	0.00	0.40	0.00	0.00	0.00	0.00	61.42	9.49	<b>94.12</b>	56.43	0.00	1.01	5.29	2.76	3.63	0.00	0.00	0.21	0.00	0.00	0.00	0.00	30.66	
1	33	16	magnetite: lamellar (mixed?)	0.00	3.10	9.25	3.59	0.78	0.00	0.17	0.84	0.00	0.00	0.00	0.00	71.39	1.91	<b>91.03</b>	55.38	0.00	2.03	5.14	1.69	0.82	0.00	0.12	0.50	0.00	0.00	0.00	0.00	34.33	
1	33	17	magnetite: lamellar (mixed?)	0.00	2.39	9.73	3.54	0.66	0.00	0.00	0.18	0.00	0.00	0.00	0.00	81.45	1.60	<b>99.56</b>	57.71	0.00	1.37	4.74	1.46	0.60	0.00	0.00	0.10	0.00	0.00	0.00	0.00	34.03	
3	12	4	magnetite: lamellar (mixed?)	0.00	4.30	8.38	2.95	2.24	0.00	0.23	0.53	0.45	0.00	0.00	0.48	75.97	5.46	<b>101.00</b>	53.63	0.00	2.58	4.26	1.27	2.13	0.00	0.15	0.29	0.17	0.00	0.00	0.21	35.30	
2	3	8	olivine	0.35	0.96	30.63	5.56	0.00	0.00	0.00	0.77	0.00	0.00	0.00	1.44	55.57	0.00	<b>95.27</b>	60.31	0.24	0.52	14.22	2.18	0.00	0.00	0.00	0.38	0.00	0.00	0.00	0.57	21.58	
3	7	1	iron sulphide	0.00	0.00	0.60	0.44	26.55	0.00	0.00	0.00	0.00	0.00	0.00	0.00	5.21	64.72	<b>97.53</b>	21.22	0.00	0.00	0.38	0.24	31.42	0.00	0.00	0.00	0.00	0.00	0.00	0.00	0.00	46.74
3	7	2	iron sulphide	0.00	0.00	1.04	0.79	28.31	0.00	0.00	0.00	0.00	0.00	0.00	0.00	-2.31	69.01	<b>96.84</b>	24.33	0.00	0.00	0.62	0.40	31.58	0.00	0.00	0.00	0.00	0.00	0.00	0.00	43.07	
3	7	3	iron sulphide	0.00	0.00	0.37	0.00	28.10	0.00	0.00	0.00	0.00	0.00	0.00	0.00	0.69	68.49	<b>97.64</b>	17.67	0.00	0.00	0.24	0.00	34.05	0.00	0.00	0.00	0.00	0.00	0.00	0.00	48.04	
3	10	1	iron sulphide	0.00	0.61	3.22	1.33	23.76	0.00	0.00	0.67	0.00	0.00	0.00	0.00	11.89	57.92	<b>99.38</b>	27.65	0.00	0.43	1.90	0.66	26.28	0.00	0.00	0.42	0.00	0.00	0.00	0.00	42.66	
3	12	2	iron sulphide	0.00	0.00	2.20	0.74	26.96	0.00	0.00	0.20	0.00	0.00	0.00	0.00	0.75	65.71	<b>96.56</b>	24.70	0.00	0.00	1.33	0.38	30.45	0.00	0.00	0.13	0.00	0.00	0.00	0.00	43.01	
1	33	10	wustite?	0.00	1.12	0.88	0.00	0.00	0.00	0.00	0.00	0.00	0.00	0.00	96.28	0.00	<b>98.28</b>	52.19	0.00	0.76	0.51	0.00	0.00	0.00	0.00	0.00	0.00	0.00	0.00	0.00	0.00	46.54	
1	33	11	wustite?	0.00	1.28	1.84	0.49	2.40	0.00	0.00	0.00	0.00	0.00	0.00	82.39	5.85	<b>94.25</b>	52.74	0.00	0.85	1.04	0.23	2.55	0.00	0.00	0.00	0.00	0.00	0.00	0.00	0.00	42.58	
1	33	12	wustite?	0.00	1.10	1.53	0.87	0.16	0.00	0.00	0.00	0.00	0.00	0.00	94.57	0.38	<b>98.61</b>	53.60	0.00	0.72	0.85	0.41	0.16	0.00	0.00	0.00	0.00	0.00	0.00	0.00	0.00	44.26	
1	33	13	wustite?	0.00	1.04	1.34	0.57	0.59	0.00	0.00	0.00	0.00	0.00	0.00	92.95	1.45	<b>97.95</b>	52.92	0.00	0.69	0.76	0.27	0.63	0.00	0.00	0.00	0.00	0.00	0.00	0.00	0.00	0.00	44.73
1	32	1	cement coat - outer	0.00	3.79	12.56	0.00	0.36	0.00	0.00	1.40	0.00	0.00	0.00	0.00	56.14	0.87	<b>75.12</b>	69.42	0.00	2.04	5.72	0.00	0.31	0.00	0.00	0.68	0.00	0.00	0.00	0.00	0.00	21.83
1	32	2	cement coat	0.00	10.91	22.51	0.47	0.38	0.00	0.20	2.20	0.00	0.00	0.00	0.00	36.92	0.93	<b>74.53</b>	70.21	0.00	5.40	9.45	0.17	0.30	0.00	0.11	0.99	0.00	0.00	0.00	0.00	0.00	13.38
1	32	3	cement coat	0.00	5.99	15.16	1.95	0.32	0.00	0.00	1.54	0.00	0.00	0.00	0.00	53.18	0.79	<b>78.94</b>	71.44	0.00	2.82	6.06	0.66	0.24	0.00	0.00	0.66	0.00	0.00	0.00	0.00	0.00	18.12
1	32	4	cement coat	0.00	1.42	12.60	4.52	0.13	0.00	0.00	2.57	0.00	0.00	0.00	0.00	55.74	0.32	<b>77.30</b>	70.19	0.00	0.73	5.52	1.68	0.11	0.00	0.00	1.21	0.00	0.00	0.00	0.00	0.00	20.57
1	32	5	cement coat - inner	0.00	0.82	11.33	3.09	0.00	0.00	0.00	1.91	0.00	0.00	0.00	0.00	61.00	0.00	<b>78.15</b>	69.56	0.00	0.43	5.07	1.17	0.00	0.00	0.00	0.92	0.00	0.00	0.00	0.00	0.00	22.85

Table 1. EDS spot microanalyses, expressed as wt% oxide, (except for sulphur as wt% element and iron, which is partitioned into wt% element on the basis all S is combined as Fe<sub>1.4</sub>S and the remainder as wt% FeO) and as normalised atom%

sample	SOI	#	phase	grain number	wt% oxide														
					Na	Mg	Al	Si	P	S	Cl	K	Ca	Ti	V	Cr	Mn	Fe <sup>II</sup>	Fe(S)
			<b>slag</b>																
LVI 2	2	20	area	grain 2-1	0.00	0.00	7.03	15.37	6.51	0.00	0.00	0.98	0.00	0.00	0.00	0.48	69.62	0.00	
LVI 1	36	5	area - large grain or slag fragment?	grain 1-1	0.00	0.00	3.24	9.26	4.40	2.30	0.00	0.71	0.00	0.00	0.00	0.00	74.48	5.61	
LVI 1	36	7	area - slag grain with cooling front	grain 1-2	0.00	0.00	6.74	8.10	4.38	0.72	0.00	2.60	0.00	0.00	0.00	0.00	75.71	1.75	
					<b>0.00</b>	<b>0.00</b>	<b>5.67</b>	<b>10.91</b>	<b>5.10</b>	<b>1.01</b>	<b>0.00</b>	<b>0.00</b>	<b>1.43</b>	<b>0.00</b>	<b>0.00</b>	<b>0.16</b>	<b>73.27</b>	<b>2.45</b>	
			<b>dense spheroids</b>																
LVI 1	34	10	area - squarish grain	grain 1-3	0.00	0.00	3.42	11.04	3.70	1.03	0.00	0.53	0.00	0.00	0.00	0.00	77.75	2.52	
LVI 1	35	4	area - outer compound grain?	grain 1-4	0.00	0.00	6.65	2.20	4.52	0.61	0.00	0.44	0.00	0.00	0.00	0.00	84.09	1.49	
LVI 1	35	9	area - bright	grain 1-5	0.00	0.00	4.20	11.81	6.01	1.62	0.00	0.36	0.00	0.00	0.32	71.72	3.96		
					<b>0.00</b>	<b>0.00</b>	<b>4.76</b>	<b>8.35</b>	<b>4.74</b>	<b>1.09</b>	<b>0.00</b>	<b>0.00</b>	<b>0.44</b>	<b>0.00</b>	<b>0.00</b>	<b>0.11</b>	<b>77.85</b>	<b>2.66</b>	
			<b>dense vesicular spheroids</b>																
LVI 3	2	2	Grain1	grain 3-1	0.00	0.00	2.99	8.36	3.58	2.23	0.00	0.15	0.50	0.00	0.00	0.47	76.28	5.43	
LVI 3	2	3	Grain1	grain 3-1	0.00	0.00	2.39	9.58	4.10	2.52	0.00	0.00	0.59	0.00	0.00	0.45	74.24	6.14	
LVI 3	4	1	Grain2	grain 3-2	0.00	0.00	4.41	11.25	4.65	1.95	0.00	0.38	1.45	0.00	0.00	0.80	70.34	4.76	
LVI 3	4	2	Grain2	grain 3-2	0.00	0.00	4.94	11.57	4.83	1.97	0.00	0.36	1.40	0.28	0.00	0.67	69.17	4.81	
LVI 3	13	2	Grain6	grain 3-6	0.00	0.00	2.70	8.94	5.62	3.57	0.00	0.00	0.57	0.00	0.00	0.00	69.91	8.69	
LVI 3	13	3	Grain6	grain 3-6	0.00	0.00	2.94	9.19	5.58	3.13	0.00	0.17	0.75	0.00	0.00	0.00	70.59	7.64	
LVI 3	13	1	Grain6	grain 3-6	0.00	0.00	3.54	8.32	4.58	2.67	0.00	0.25	0.86	0.00	0.00	0.00	73.28	6.50	
LVI 1	34	1	area - upper right grain	grain 1-6	0.00	0.00	3.45	9.90	4.38	2.31	0.00	0.18	0.72	0.00	0.00	0.47	72.98	5.63	
LVI 1	34	2	area - upper right grain	grain 1-6	0.00	0.00	3.54	10.65	4.57	2.27	0.00	0.27	0.73	0.00	0.00	0.00	72.43	5.54	
LVI 1	34	3	area - upper right grain	grain 1-6	0.00	0.00	3.32	10.49	4.55	1.26	0.00	0.00	0.41	0.00	0.00	0.00	76.90	3.08	
LVI 1	34	4	area - lower centre grain	grain 1-7	0.00	0.00	3.87	12.83	4.98	0.84	0.00	0.00	0.54	0.00	0.00	0.58	74.29	2.06	
LVI 1	34	5	area - lower centre grain	grain 1-7	0.00	0.00	4.15	12.22	4.55	2.33	0.00	0.28	0.86	0.00	0.00	0.47	69.47	5.67	
LVI 1	35	1	area - upper left grain	grain 1-8	0.00	0.00	4.98	14.19	4.93	2.66	0.00	0.44	0.61	0.00	0.00	0.42	65.27	6.49	
LVI 1	35	5	area - inner compound grain?	grain 1-9	0.00	0.00	4.45	14.37	4.73	2.68	0.00	0.00	0.46	0.00	0.00	0.35	66.43	6.53	
LVI 3	6	1	Grain3	grain 3-3	0.00	0.00	3.37	6.93	4.91	0.98	0.00	0.00	0.38	0.00	0.00	0.35	81.09	2.00	
LVI 3	6	2	Grain3	grain 3-3	0.00	0.00	2.55	7.32	5.17	3.35	0.00	0.00	0.36	0.00	0.00	0.36	74.04	6.86	
					<b>0.00</b>	<b>0.00</b>	<b>3.60</b>	<b>10.38</b>	<b>4.73</b>	<b>2.30</b>	<b>0.00</b>	<b>0.16</b>	<b>0.70</b>	<b>0.02</b>	<b>0.00</b>	<b>0.34</b>	<b>72.29</b>	<b>5.49</b>	
			<b>thin shell spheroids</b>																
LVI 1	36	1	area - central grain	grain 1-10	0.00	0.00	4.14	10.43	5.09	1.68	0.00	0.00	0.33	0.00	0.00	0.00	74.22	4.11	
LVI 1	36	6	area - centre lower grain	grain 1-11	0.00	0.00	2.76	9.83	5.15	2.95	0.00	0.00	0.79	0.00	0.00	0.43	70.90	7.20	
LVI 1	36	8	area - lower left grain	grain 1-12	0.00	0.00	5.31	3.60	0.50	1.99	0.00	0.00	0.00	0.00	0.00	0.00	83.74	4.86	
LVI 3	8	1	Grain4	grain 3-4	0.00	0.00	4.44	10.91	4.04	2.10	0.00	0.29	1.53	0.00	0.00	0.51	71.07	5.12	
LVI 3	8	2	Grain4	grain 3-4	0.00	0.00	5.86	11.13	4.07	2.06	0.00	0.34	1.40	0.00	0.00	0.35	69.76	5.03	
LVI 1	34	6	area - lower right grain	grain 1-13	0.00	0.00	2.92	12.27	6.45	1.57	0.00	0.00	0.46	0.28	0.00	0.35	71.87	3.83	
LVI 1	34	7	area - lower right grain	grain 1-13	0.00	0.00	3.28	11.98	5.99	3.03	0.00	0.00	0.45	0.00	0.00	0.00	67.88	7.40	
LVI 1	34	8	area - mid left grain	grain 1-14	0.00	0.00	3.77	8.23	4.20	1.62	0.00	0.00	0.64	0.00	0.00	0.00	77.60	3.94	
LVI 1	34	9	area - mid left grain	grain 1-14	0.00	0.00	3.34	9.53	4.74	1.70	0.00	0.00	0.64	0.00	0.00	0.00	75.90	4.14	
LVI 1	35	2	area - centre left grain	grain 1-15	0.00	0.00	3.52	10.33	5.57	1.03	0.00	0.00	0.54	0.00	0.00	0.00	76.49	2.52	
LVI 3	11	1	Grain5	grain 3-5	0.00	0.00	4.94	9.43	4.31	2.84	0.00	0.18	0.94	0.00	0.00	0.63	69.81	6.92	
					<b>0.00</b>	<b>0.00</b>	<b>4.03</b>	<b>9.79</b>	<b>4.56</b>	<b>2.05</b>	<b>0.00</b>	<b>0.07</b>	<b>0.70</b>	<b>0.03</b>	<b>0.00</b>	<b>0.21</b>	<b>73.57</b>	<b>5.01</b>	
			<b>flake</b>																
LVI 1	34	14	area - bright scale fragment?	grain 1-16	0.00	0.00	1.23	3.05	0.91	0.13	0.00	0.00	0.00	0.00	0.00	0.00	94.34	0.33	
LVI 1	36	2	area - bright scale fragment?	grain 1-17	0.00	0.00	1.23	1.31	0.44	0.21	0.00	0.00	0.00	0.00	0.00	0.44	95.86	0.51	
LVI 1	36	3	area - bright scale fragment?	grain 1-18	0.00	0.00	0.58	0.56	0.00	0.14	0.00	0.00	0.00	0.00	0.00	0.00	98.37	0.35	
LVI 1	36	4	area - bright scale fragment?	grain 1-19	0.00	0.00	1.38	1.15	0.00	0.19	0.00	0.00	0.19	0.00	0.00	0.00	96.62	0.47	
					<b>0.00</b>	<b>0.00</b>	<b>1.11</b>	<b>1.52</b>	<b>0.34</b>	<b>0.17</b>	<b>0.00</b>	<b>0.00</b>	<b>0.05</b>	<b>0.00</b>	<b>0.00</b>	<b>0.11</b>	<b>96.30</b>	<b>0.42</b>	
			<b>weathering</b>																
LVI 1	35	7	area - dark		0.30	0.91	30.66	54.61	1.23	0.40	0.17	2.04	0.54	0.82	0.00	0.00	0.00	7.33	0.98

sample	SOI	#	phase	grain number	wt% oxide														
					Na	Mg	Al	Si	P	S	Cl	K	Ca	Ti	V	Cr	Mn	Fe	Fe(S)
			<b>cement</b>																
LVI 1	34	13	area - cement		0.00	0.00	0.81	1.10	0.00	0.27	0.00	0.00	0.00	0.00	0.00	0.00	0.00	97.16	0.66
LVI 1	35	3	area - cement		0.00	0.00	1.08	1.05	1.18	0.58	0.00	0.00	0.00	0.00	0.00	0.00	0.00	94.67	1.42
LVI 1	35	6	area - cement		0.00	0.00	0.73	0.79	1.57	0.42	0.00	0.00	0.00	0.00	0.00	0.00	0.00	95.46	1.02
			<b>fuel</b>		0.00	0.00	0.87	0.98	0.92	0.42	0.00	0.00	0.00	0.00	0.00	0.00	0.00	95.76	1.03
LVI 1	34	12	area - fuel fragment		0.00	0.00	41.92	52.14	0.60	0.38	0.00	0.46	0.54	0.00	0.00	0.00	0.00	3.04	0.92

Table 2: normalised EDS area analyses, expressed as wt% oxide, except for sulphur (wt% element) and iron, which is partitioned into wt% element on the basis all S is combined as  $Fe_{1.4}S$  and the remainder as wt% FeO.

Source			Analysis (oxides)										(sulphide)		iron sulphide	Al <sub>2</sub> O <sub>3</sub> : SiO <sub>2</sub>
			Na	Mg	Al	Si	P	K	Ca	Ti	Mn	Fe	S	Fe		
This study		average of EDS areas in spheroids, LVI-1 and LVI-3	0.00	0.00	3.87	9.96	4.67	0.11	0.67	0.02	0.27	73.32	2.09	5.03	7.12	0.39
This study		XRF of bulk spheroids, LVI-3	0.14	0.11	3.55	9.64	3.80	0.30	1.58	0.24	0.43	69.13	3.24	7.80	11.04	0.37
This study		EDS area of slag, LVI-2	0.00	0.00	7.03	15.37	6.51	0.00	0.98	0.00	0.48	69.62	0.00	0.00	0.00	0.40
Percy, 1864	1	Dowlais Ironworks, white pig														
Percy, 1864	1	Dowlais Ironworks, white pig														
Percy, 1864	2	Dowlais, with limestone boshes														
Percy, 1864	3	Dowlais, with red ore boshes														
Percy, 1864	4	Bromford Ironworks														
Percy, 1864	5	bulldog, Bloomfield Ironworks														
Percy, 1864	6	Chillington Ironworks														
Stansbie, 1907		boilings														
Stansbie, 1907		tappings														
MacFarlane 1917		Boilings														
MacFarlane 1917		Average tap														
Hearson, 1922		best tap														
Hearson, 1922		bulldog														
Killick & Gordon 1987	A	Fontley														
Killick & Gordon 1987	D	Roxbury, USA														

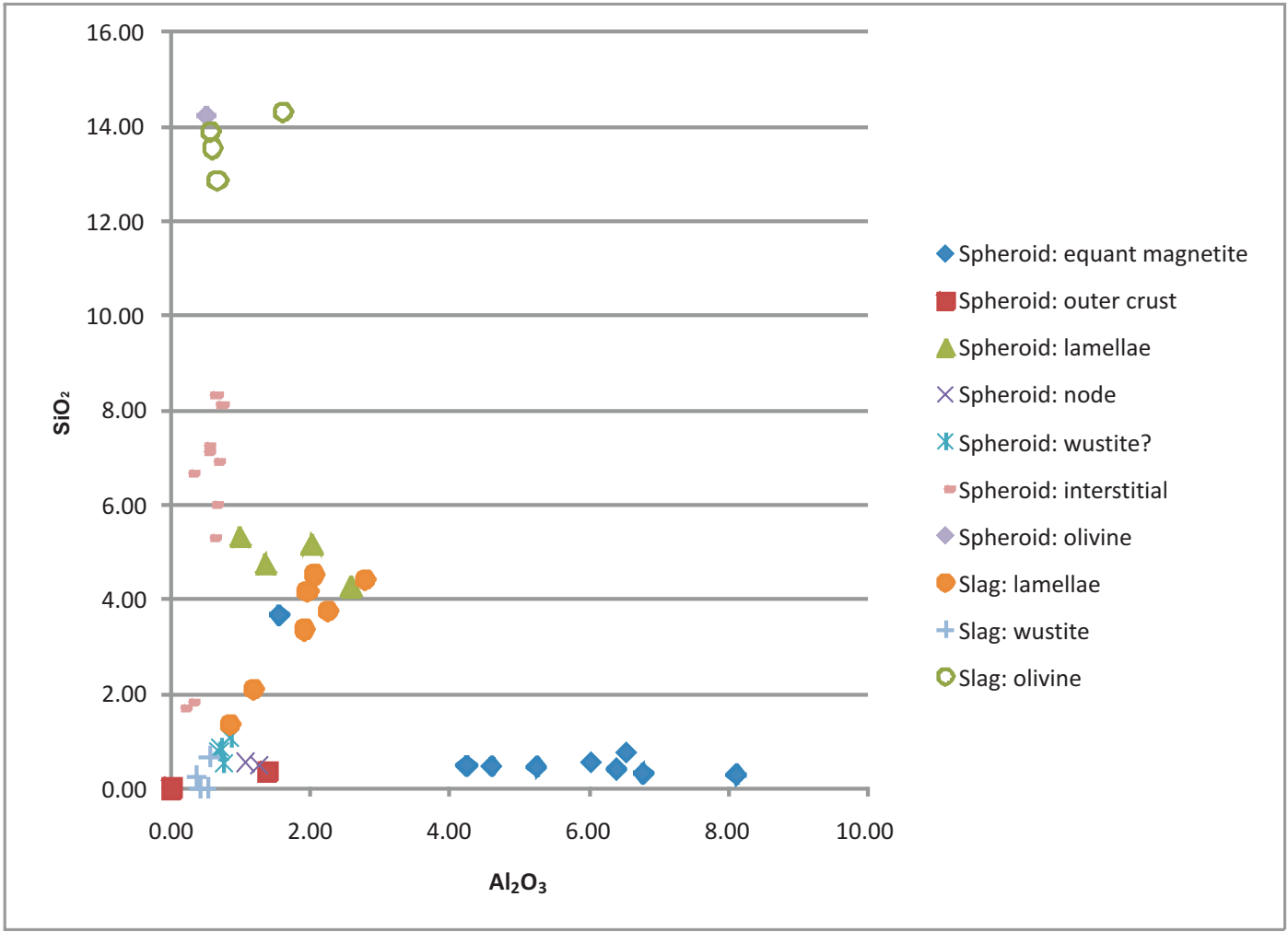
Table 3: bulk composition of spheroidal hammerscale from Llynfi Vale Ironworks, estimated from average EDS area analysis and by XRF of bulk sample, compared with other early analyses of puddling slags (Percy), textbook "typical" values (Stansbie, MacFarlane and Harson) and modern analyses (Killick & Gordon).

a)	SiO <sub>2</sub>	Al <sub>2</sub> O <sub>3</sub>	Fe <sub>2</sub> O <sub>3</sub>	FeO	MnO	MgO	CaO	Na <sub>2</sub> O	K <sub>2</sub> O	TiO <sub>2</sub>	P <sub>2</sub> O <sub>5</sub>	LOI	LOI	total	%S				
	8.78	3.46	79.90	71.91	0.394	0.10	1.47	0.13	0.27	0.217	3.458	-2.4	5.59	95.78	2.94				
b)	Sc	V	Cr	Co	Ni	Cu	Zn	Ga	Rb	Sr	Y	Zr	Nb	Mo	Sn	Cs	Ba		
	4.1	290.2	234.5	12.6	18.9	86.8	84.6	37.4	11.7	38.2	6.2	26.8	24.30	1.74	1.17	0.97	82.6		
c)	La	Ce	Pr	Nd	Sm	Eu	Gd	Tb	Dy	Ho	Er	Tm	Yb	Lu	Hf	Ta	Pb	Th	U
	7.10	14.87	1.71	6.05	1.25	0.28	1.09	0.18	0.97	0.17	0.53	0.08	0.54	0.08	0.65	0.90	3.17	2.14	0.71

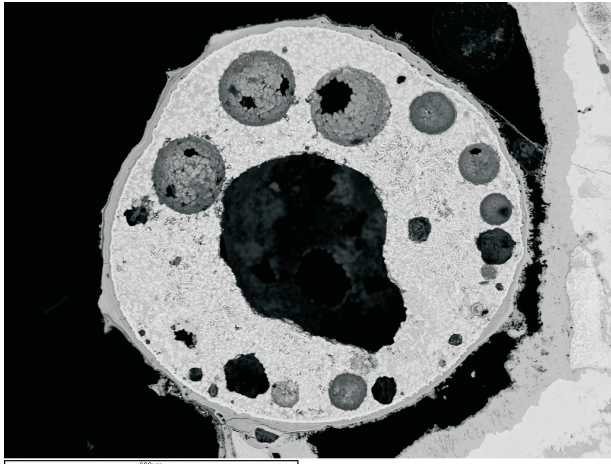
Table 4: bulk composition of isolated spheroidal hammerscale from Llynfi Vale Ironworks

a) major elements by XRF as wt% oxides, Fe calculated as either FeIII or as FeII (shaded). LOI = loss on ignition. Wt% S is also shown, but is analysed with lower precision.

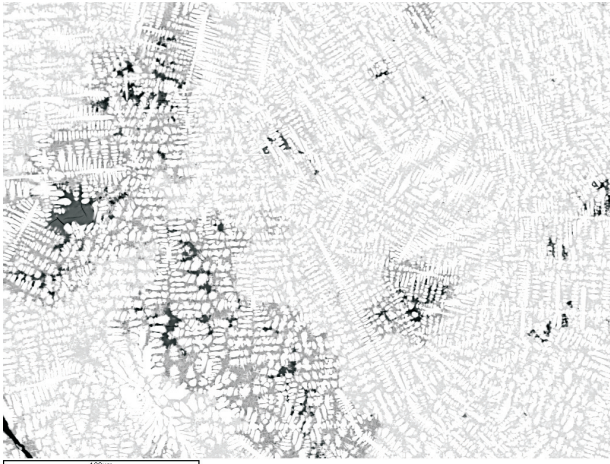
b) and c) trace elements by ICP-MS in ppm.



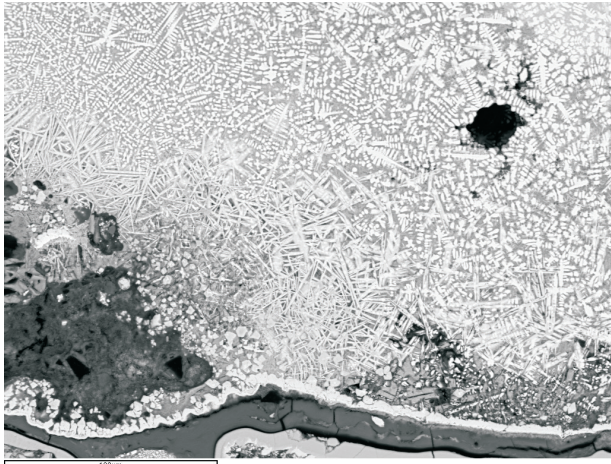
a



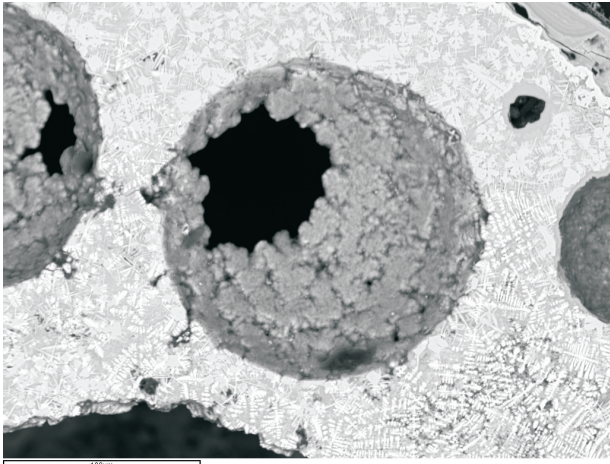
b



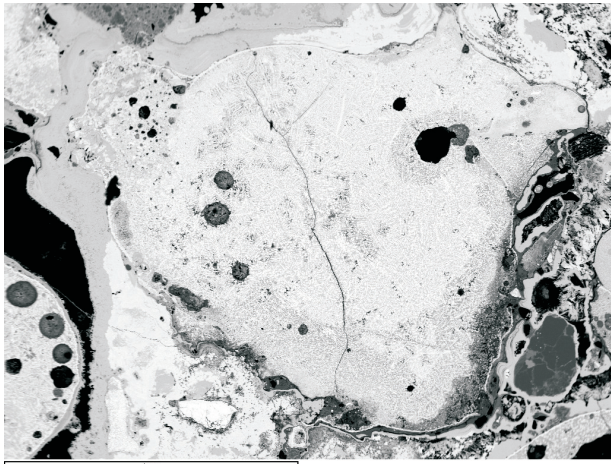
c



d



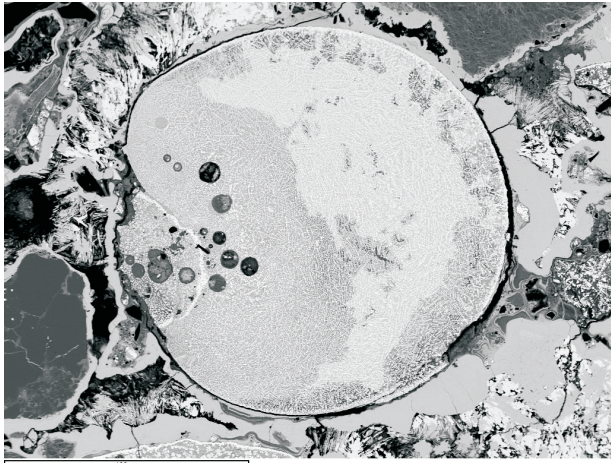
e



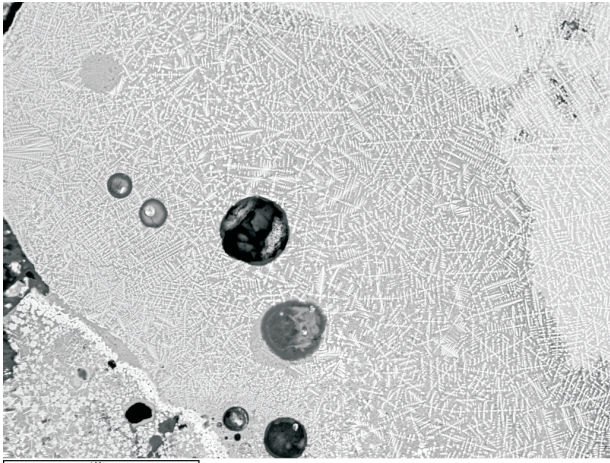
f



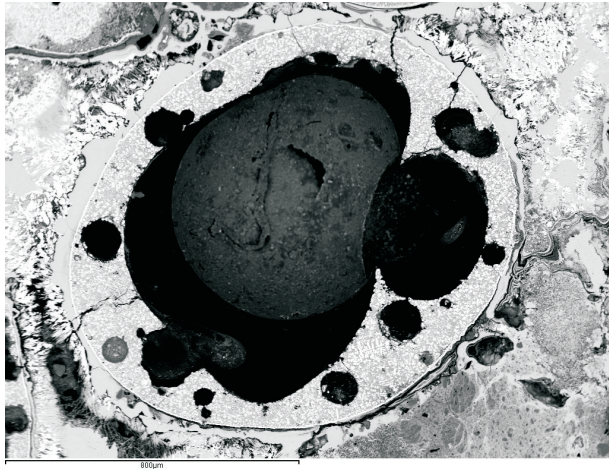
g



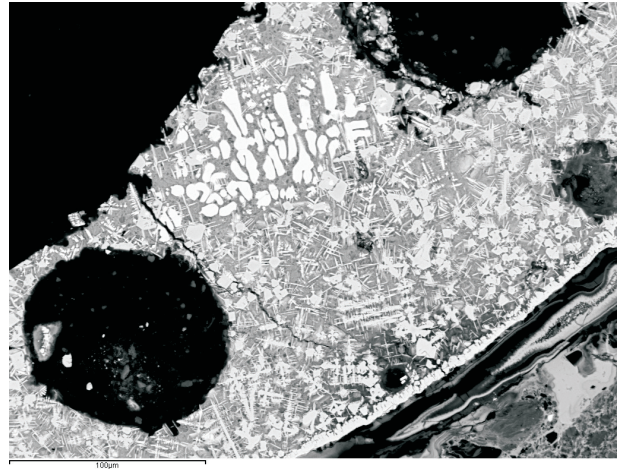
h



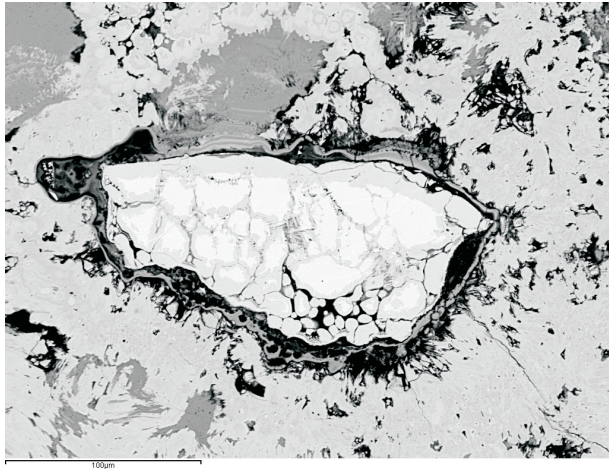
a



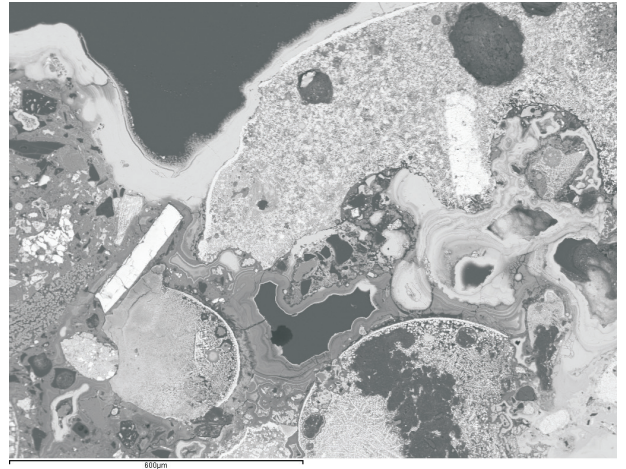
b



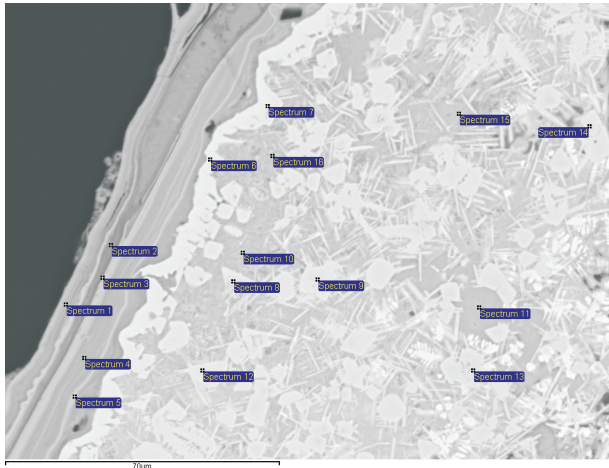
c



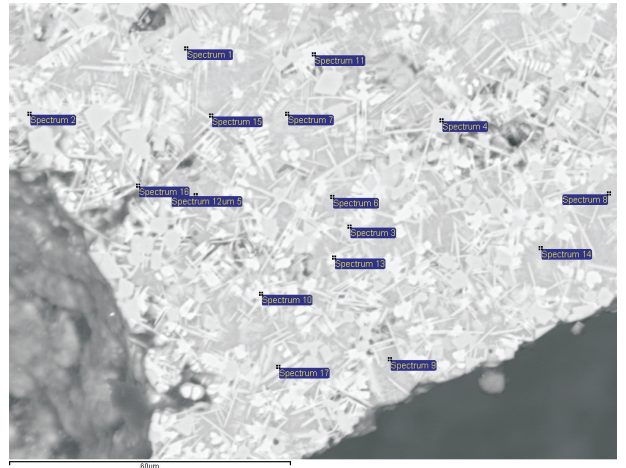
d



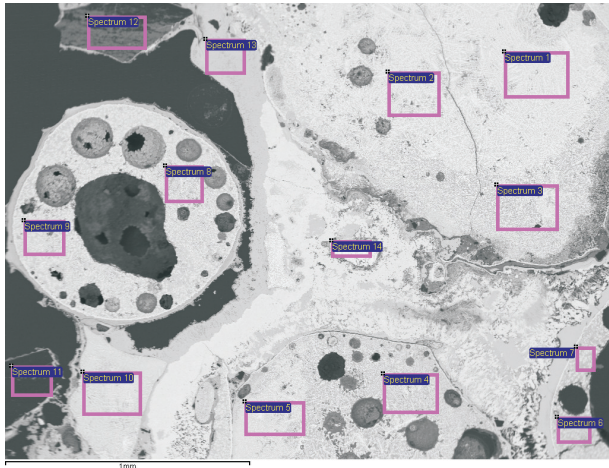
e



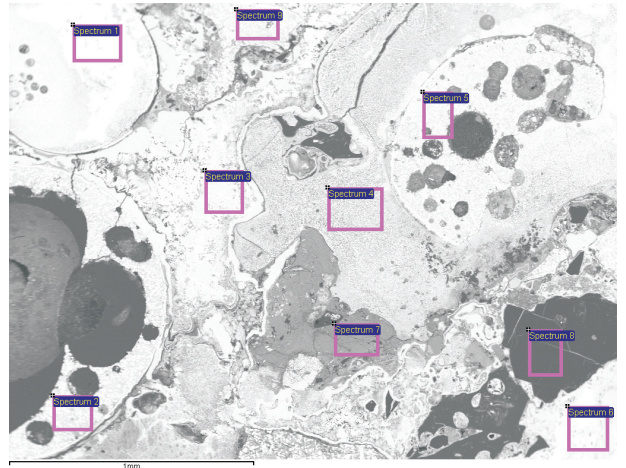
f



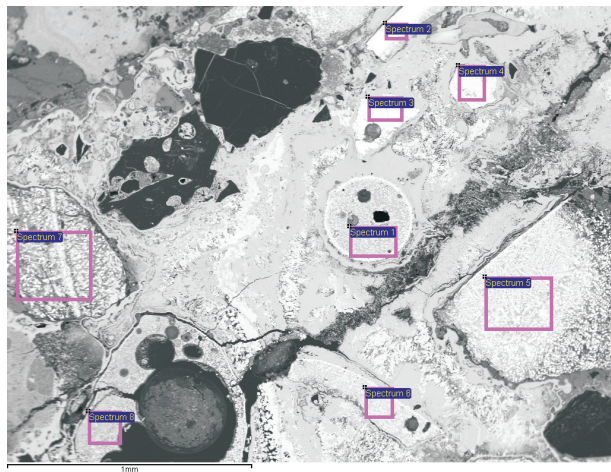
g



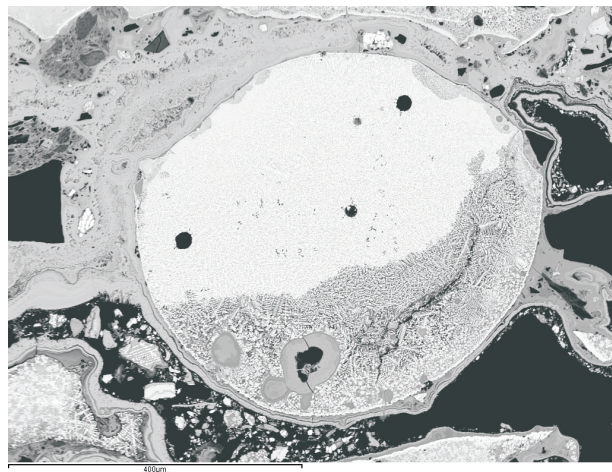
h



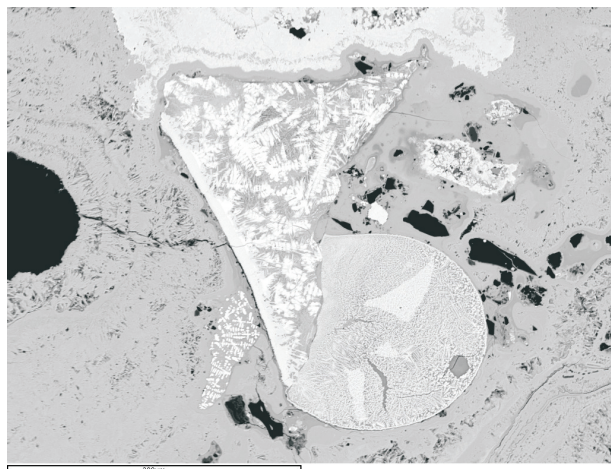
a



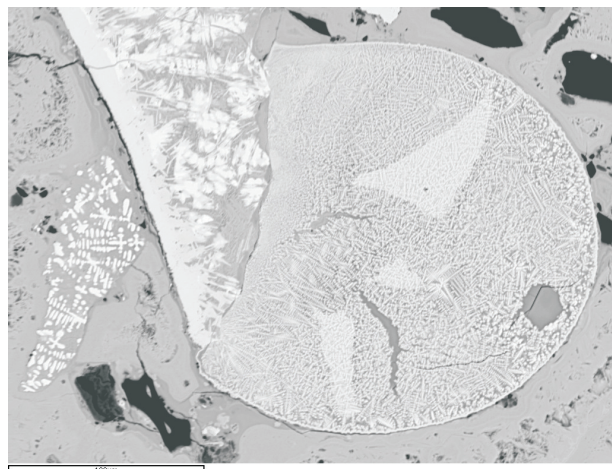
b



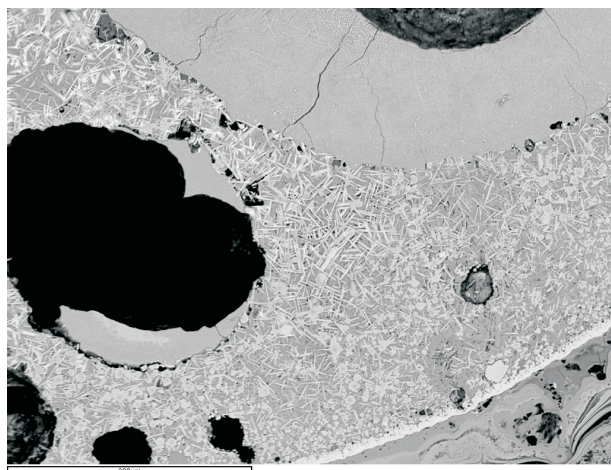
c



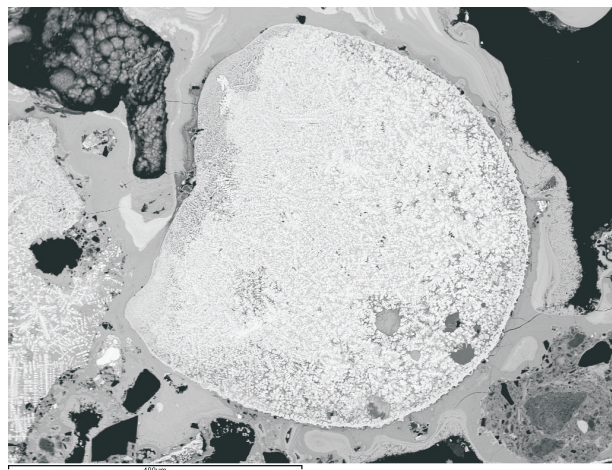
d



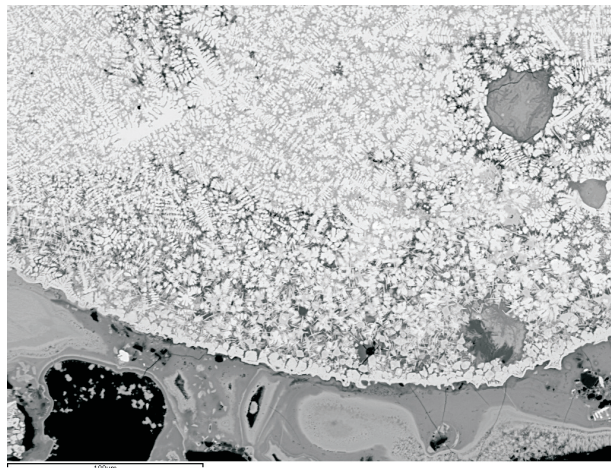
e



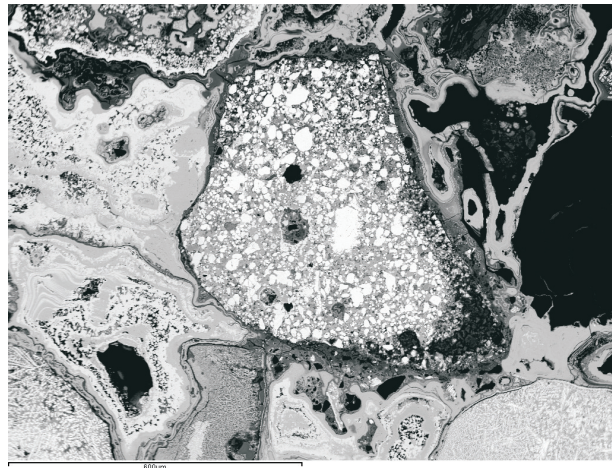
f

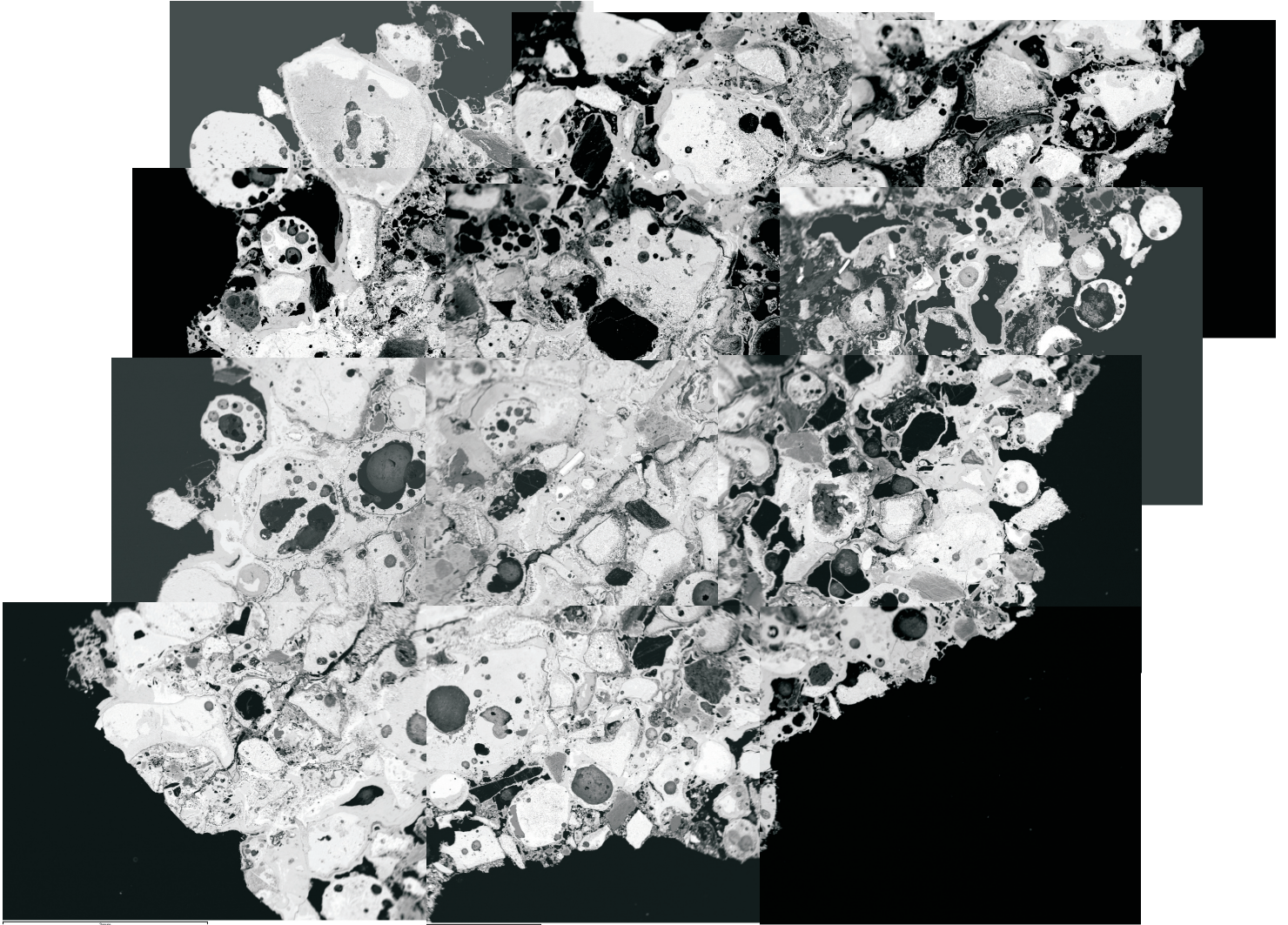


g

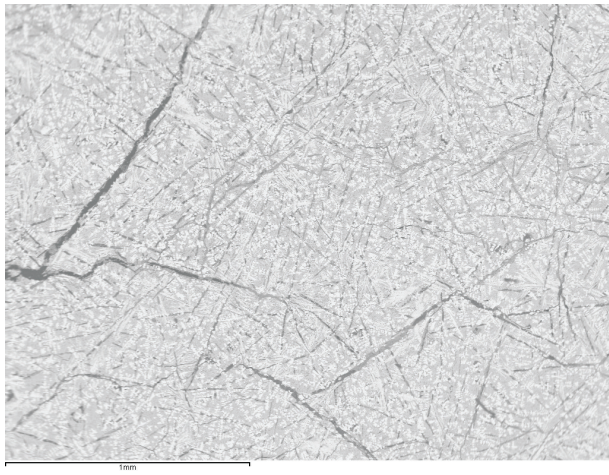


h

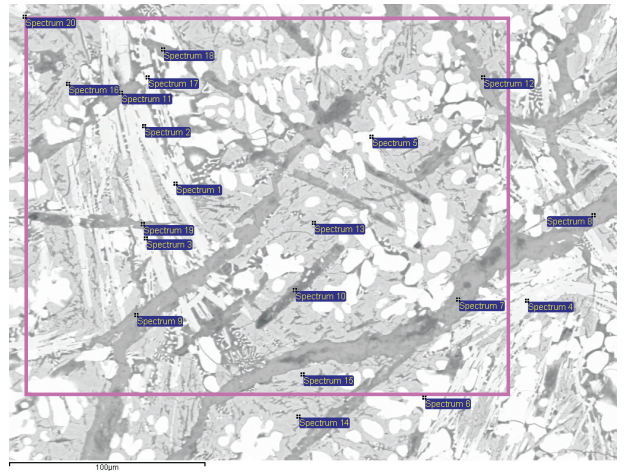




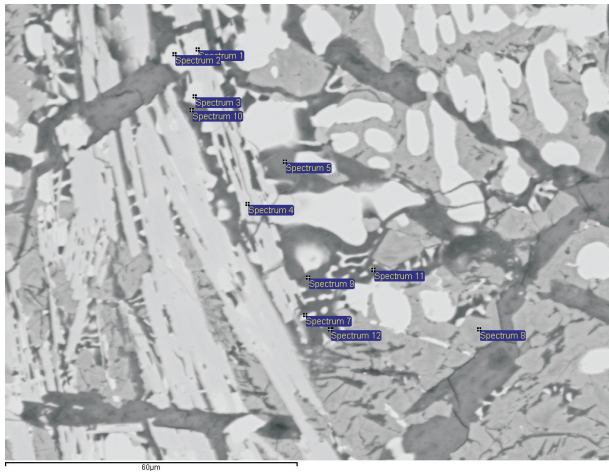
a



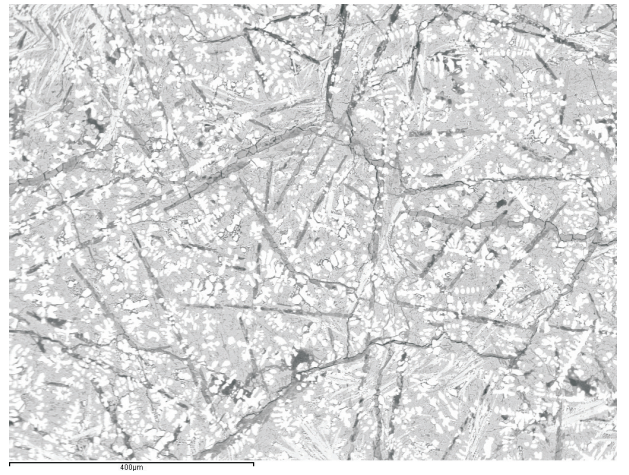
b



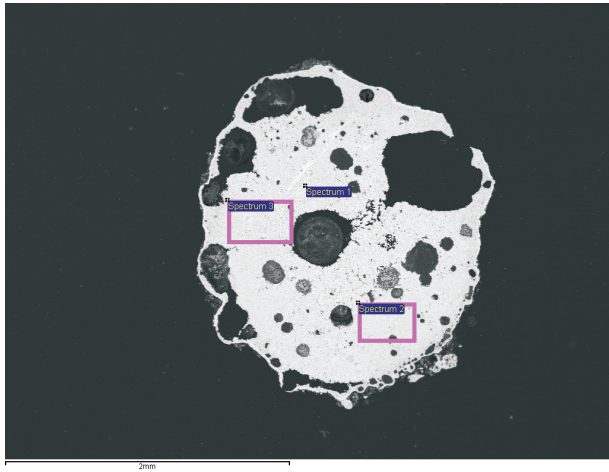
c



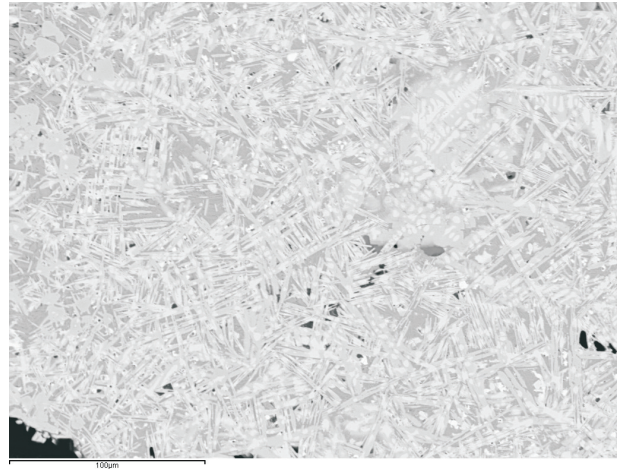
d



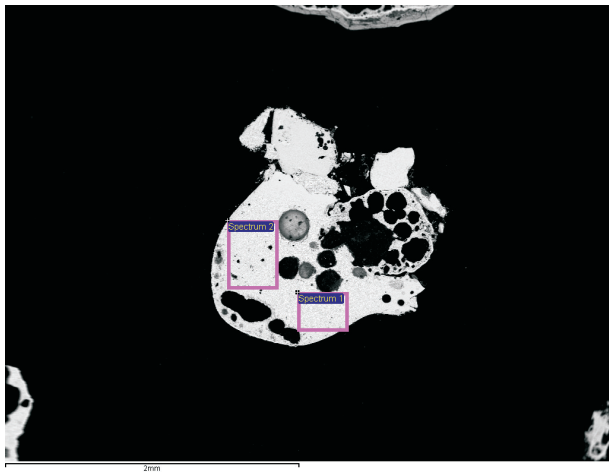
a



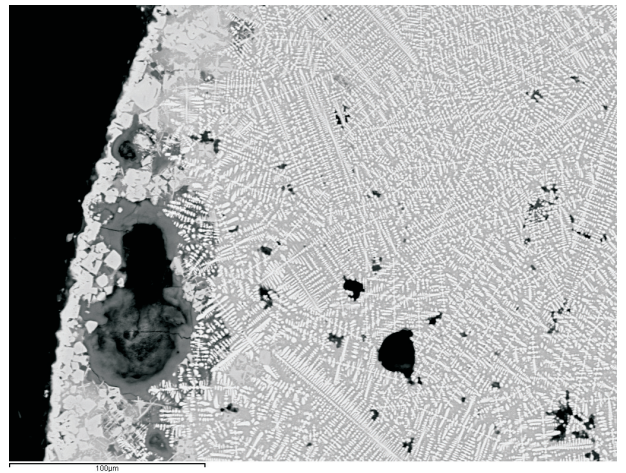
b



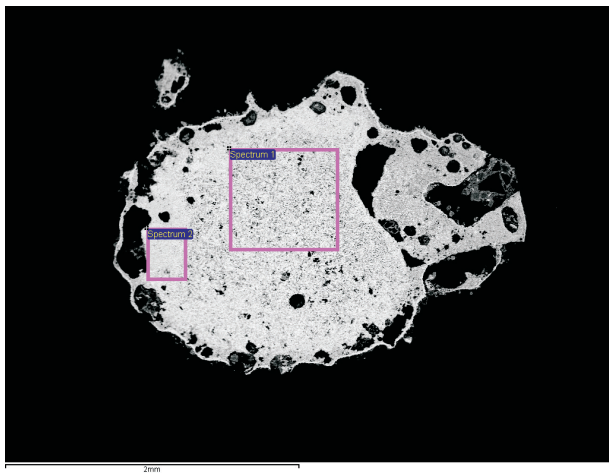
c



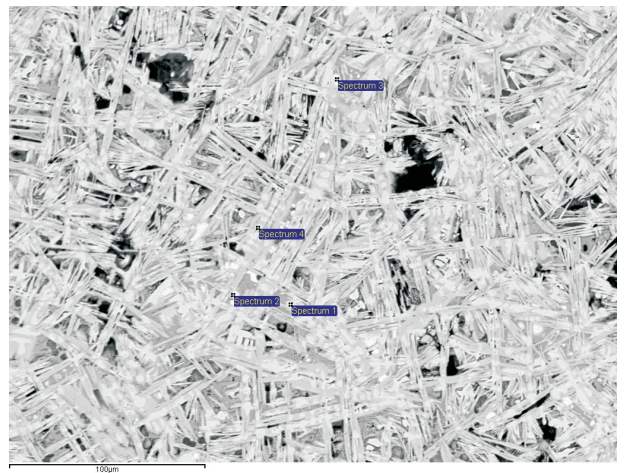
d



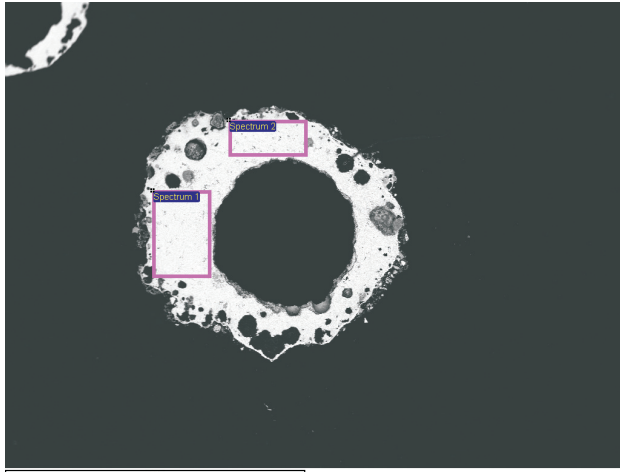
e



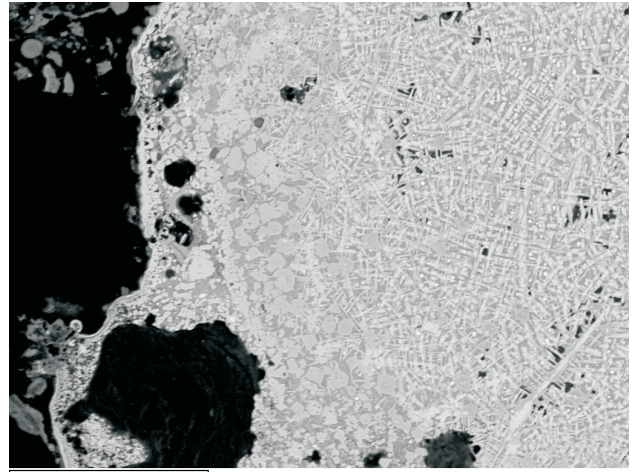
f



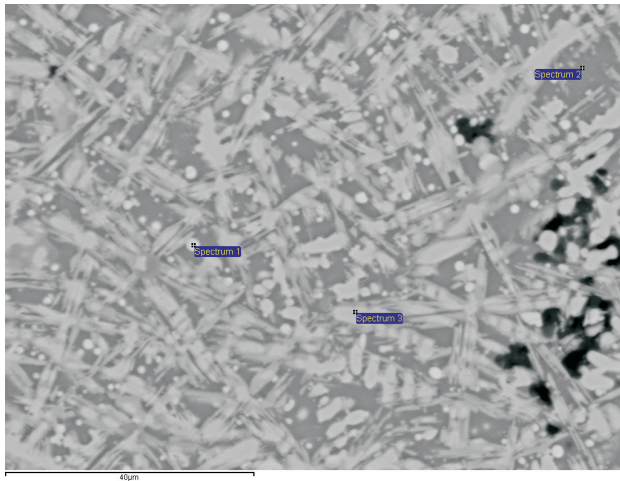
g



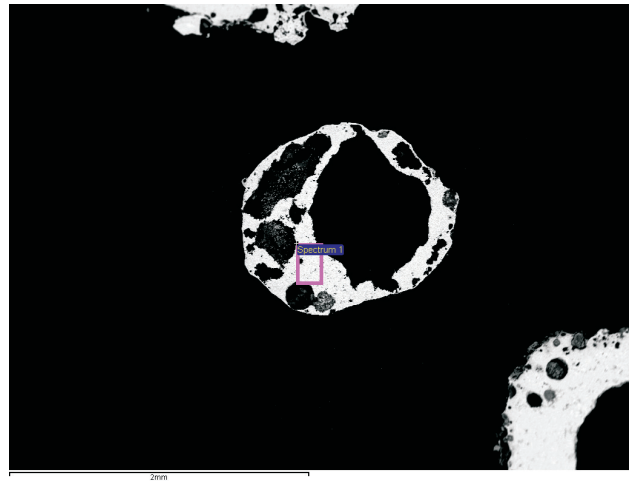
h



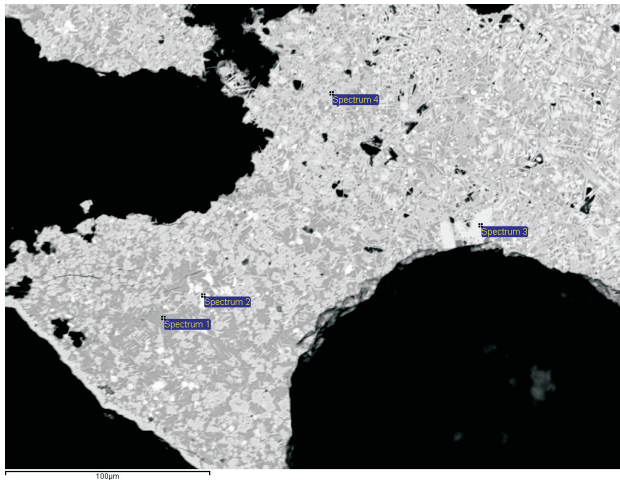
a



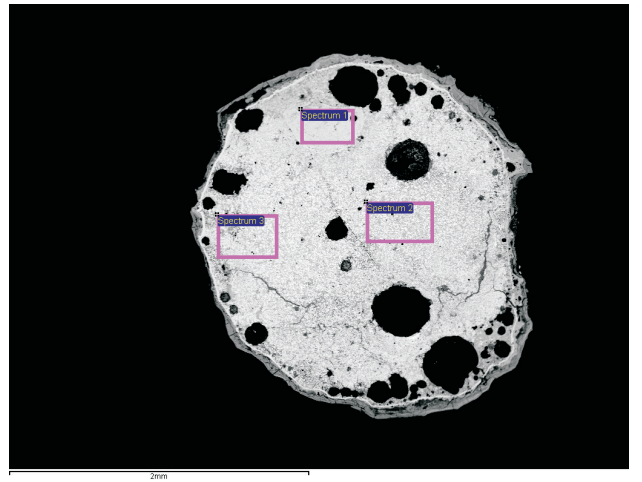
b



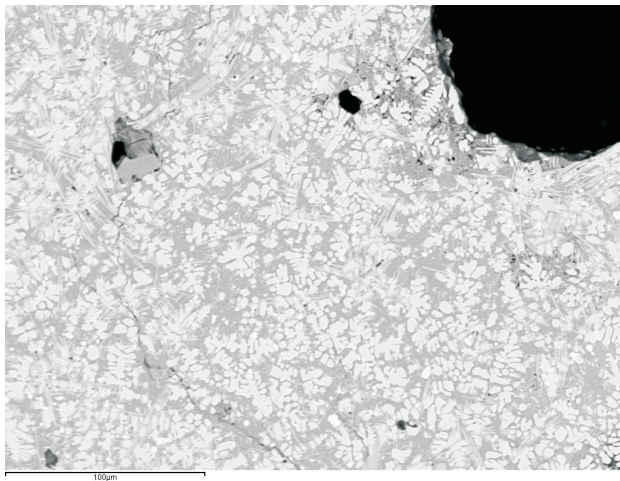
c



d



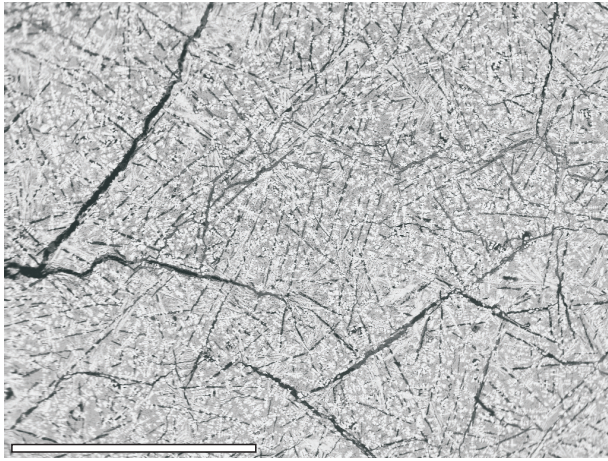
e



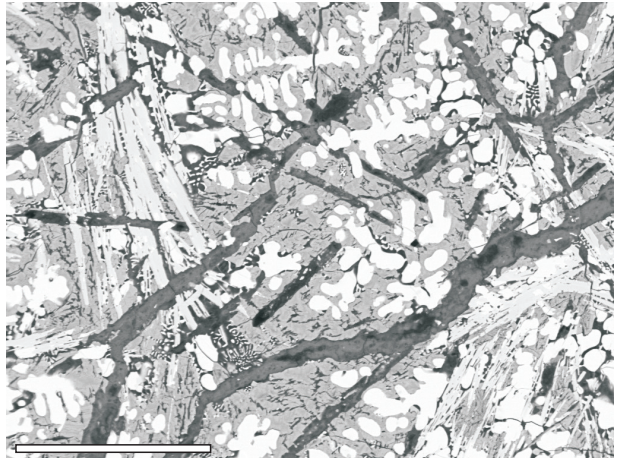
f



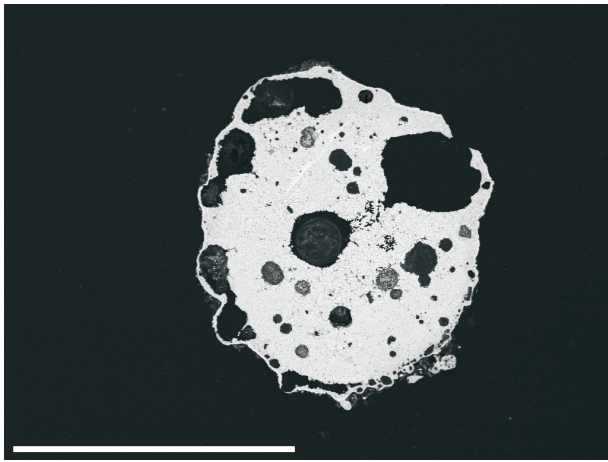
a



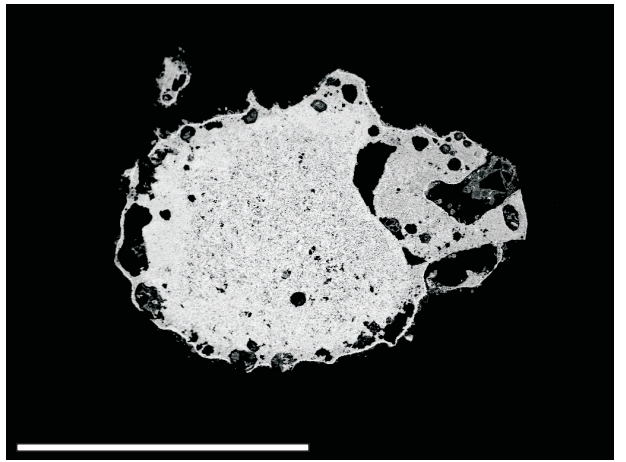
b



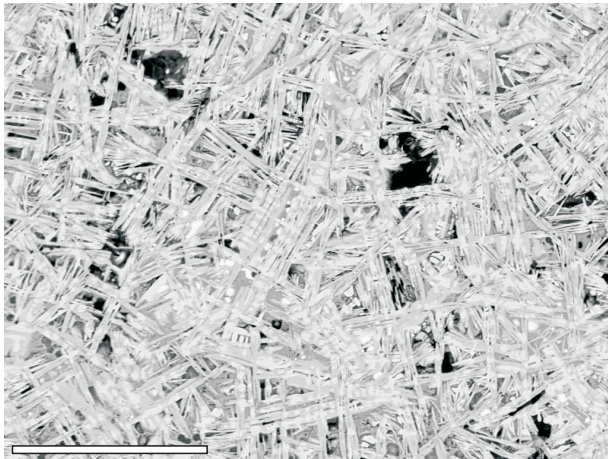
c



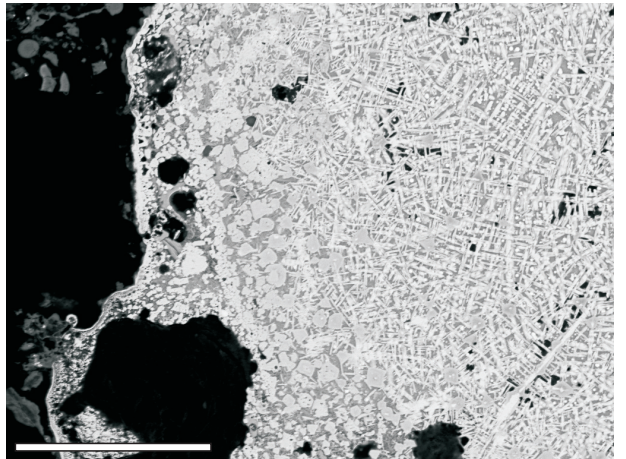
d



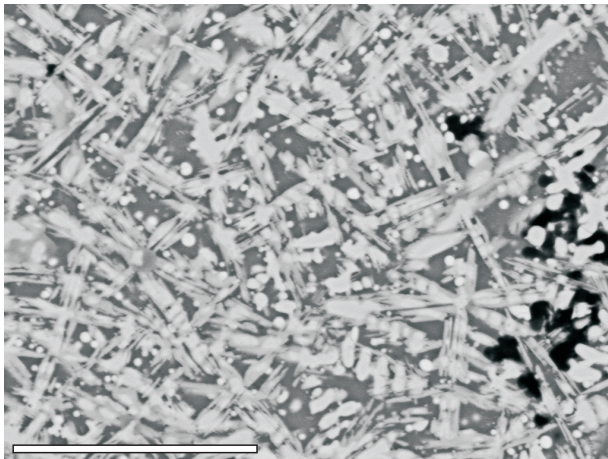
e



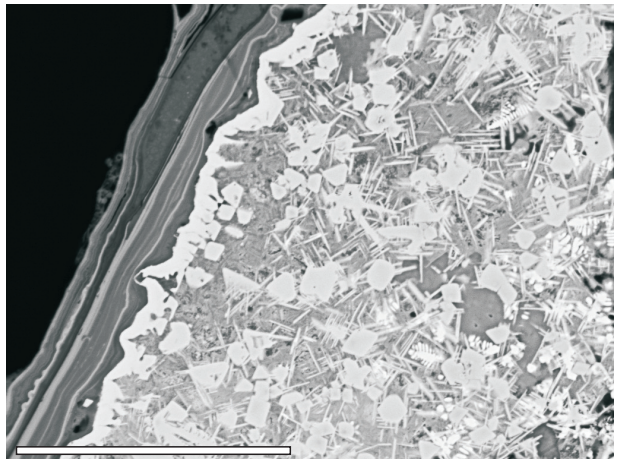
f



g



h



# GeoArch



*geoarchaeological, archaeometallurgical & geophysical investigations*

54 Heol y Cadno,  
Thornhill,  
Cardiff,  
CF14 9DY.

*Mobile:*  
*Fax:*  
*E-Mail:*  
*Web:*

07802 413704  
08700 547366  
Tim.Young@GeoArch.co.uk  
www.GeoArch.co.uk